MINISTRY OF EDUCATION AND SCIENCE OF UKRAINE

National Aerospace University
«Kharkiv Aviation Institute»

Faculty of Aircraft Engineering

Airplane and Helicopter Design Department

Explanatory Note
to Diploma Project of

Master
(degree)

Subject: Supersonic business jet general design and aerodynamic characteristics CFD study (Загальне проєктування надзвукового літака бізнес класу і CFD-дослідження його аеродинамічних характеристик)

XAI.103.161fd. 23S. 134. 10032804 EN

Applicant of 2 Year 161fd Group
Field of knowledge *13 Mechanical Engineering*
Specialty: *134 Aerospace Engineering*
Educational program: Aircraft Designing

Liu Kunhao
(name)
Supervisor: Oleksandr SOBOLIEV

(name)
Reviewer Oleksandr KOSTENKO

(name)

Kharkiv – 2023

Ministry of Science and Education of Ukraine
National Aerospace University
«Kharkiv Aviation Institute»

Faculty *Aircraft Engineering*
Department *103 Airplane and Helicopter Design*
Degree *Master*
Field of knowledge *13 Mechanical Engineering*
Specialty *134 Aerospace Engineering*
(Code and name)
Educational Program Aircraft Designing
(Name)

APPROVED by
Head of Chair
PhD, Ass. Prof. Andrii HUMENNYI
"____" _____2023___

TASK

FOR DIPLOMA PROJECT

Liu Kunhao
(Name)
Subject of qualification paper Supersonic business jet general design and aerodynamic characteristics CFD study (Загальне проєктування надзвукового літака бізнес класу і CFD-дослідження його аеродинамічних характеристик)

Supervisor of qualification paper Oleksandr SOBOLIEV
(name, degree, scientific degree)
Approved by University order No___ from "___"_____2023__
Qualification paper presentation deadline
Initial data for the qualification purpose – supersonic business jet; flight range – 6000 km; number of passengers – 10 people; takeoff distance – 2100 m; cruise speed – 2000 km/hr; cruise altitude –30 km.

Content of explanatory note (list of problems to solve)

INTRODUCTION

1 DESIGN SECTION

1.1 DESIGN REQUIREMENT

1.2 MAIN PARAMETERS ESTIMATION

Advisors of diploma project sections

Section	Name and duty of advisor	Signature, Date	
		Task is given	Task is submitted
1	**Oleksandr SOBOLIEV, Senior lecturer**	**14.03.2023**	**18.05.2023**
2	**Tetiana PAVLENKO, PhD, Ass. Prof.**	**14.03.2023**	**18.05.2023**
3	**Oleksandr SOBOLIEV, Senior lecturer**	**14.03.2023**	**18.05.2023**

Normative inspection **Oleksandr SOBOLIEV** «_18___» _____05_____2023
(Signature) (Name)

Date when task is given **14.03.2023**

CALENDAR PLAN

№	Diploma project milestones	Diploma project milestone deadlines	Notes
1	**Design Part**	**10.04.2023**	
2	**Economics**	**5.05.2023**	
3	**Special task**	**18.05.2023**	

Applicant _____ Liu Kunhao
(Signature) (Initials and surname)

Supervisor of diploma project _____ **Oleksandr SOBOLIEV**
(Signature) (Initials and surname)

Abstract

Assignment for diploma project: 104 pages, 49 figures, 19 tables, 32 sources.

Object of study: The general design of a supersonic business jet

The purpose of the work is to analyze the design features and reliability of the supersonic business jet, also called SSBJ, design its general view, load carrying structure, calculate the aerodynamic and flight characteristics of the aircraft. And through CFD software finite element analysis, the aerodynamic characteristics of the simulation.

Methods of analysis – According to the existing prototype, the requirements of the designed supersonic business jet are put forward. According to the design requirements, the overall layout design, wing design, control surface design and landing gear design of supersonic business aircraft are completed by theoretical calculation. Then the three-dimensional model was constructed by Siemens NX, the finite element processing software was used to construct the mesh of the three-dimensional model, and finally the aerodynamic characteristics of the three-dimensional model were calculated by Fluent software.

Diploma project result: The following results are obtained as a result of the Master graduation work:

The statistics were collected and processed. The aerodynamic scheme of the supersonic business jet is selected; the general layout of the aircraft is formed. The take-off mass is 40000 kg, the flight range is 6000 km, the number of passengers is 10. Structural and power scheme is developed. The aerodynamic characteristics are calculated. Cruising speed at an altitude of 30 km is M1.7.

After the finite element analysis of the aircraft take-off state, subsonic cruise state, cruise state three states, and through FLUENT simulation, the conclusion is that the aircraft designed in this paper is reliable.

In the economy part, the approximate cost of a full ticket for this SSBJ is $9,600.

Keywords: Supersonic cruise; Sonic boom; Lift-drag ratio; Business jet

Main symbol comparison table

λ	Aspect ratio	m_0	take-off weight
Ma	Mach number	$m_{0\,max}$	Max take-off weight
S	Wing area	m_f	Fuel weight
V	Flight speed	H_{cr}	Cruising altitude
W/S	Wing load	χ	Sweep Angle
C_d	Drag coefficient	η	Root-tip ratio
C_l	Lift coefficient	N-S	Navier-Stokes
K	Lift-drag ratio	deg	Angle of attack

CONTENTS

Introduction

What is a supersonic business jet

As aircraft design techniques have improved, modern subsonic transport aircraft have been able to fly great distances at cruising Mach numbers as high as 0.85. For example, the Boeing 747-400 has a maximum range of over 7,000 nautical miles. However, that distance would require the plane to be in the air for about 15 hours, or as much as 18 hours for a longer distance, such as from New York to Sydney, Australia. For civilian transport aircraft, passengers will feel very tired. However, the use of supersonic cruise passenger aircraft can be a good solution to this problem.

The supersonic cruise capability means that the aircraft can continuously fly supersonic without opening the afterburner of the engine. Current non-supersonic cruise aircraft can only go supersonic when the afterburner is turned on, and fuel consumption will soar, supersonic flight time is only a few minutes, and maneuverability is poor. The aircraft with supersonic cruise capability can overcome these deficiencies.[1] In order to realize supersonic cruise, all aviation powers have made unremitting efforts. In 1960, Britain and France cooperated in the development of supersonic passenger aircraft - "Concorde" aircraft, at the same time, the former Soviet Union developed supersonic passenger aircraft - Tupolev Tu-144. In 2010, Lockheed Martin designed a plane for NASA called Green Ultrasound. It can be seen that the love of the world's major aviation countries on supersonic cruise passenger aircraft.

Business aviation is a mode of transportation in the administrative affairs of government and various organizations and business activities. In the last 20 years of human flight, business aviation has been the most rapid development, becoming the most perfect way for people to travel by air. Business jets tend to be light and small aircraft, covering almost everything from turboprops, to medium and super-medium, to large cabins and ultra-long range jets, and even helicopters. In recent years, there has been a trend toward larger business jets, and some engineers are considering developing supersonic business jets.

There are various options for enterprises and organizations to own and use business jets: they can own them independently and set up a flight department within the

organization; Or it can be owned jointly by several companies, managed and operated by "part-owned" companies; Or by charter companies and aircraft rental companies to provide business flights.

Over the past two decades, the business aviation market has grown exponentially, even as the traditional general aviation market has declined, and especially since the COVID-19 outbreak, the preference for business aviation has reached an unexpected level.

Since the outbreak of COVID-19, many companies and individuals have put more value on safe travel, and corporations and wealthy people are less inclined to fly by airlines. Secondly, there has been a sharp decrease in flights and choice around the world, which has led to a huge growth in business aviation. On the one hand, the number of business jet deliveries has increased dramatically year by year. On the other hand, the value of the unit price aircraft has increased even more dramatically, especially with the introduction of long-range, large-cabin business jets. When fully equipped, a business jet can cost more than $50 million. All the more reason to believe that, for businessmen who believe that time is money, it is enough to justify a supersonic executive jet that can cost as much as $80 million.[2]

This belief is not unfounded, and there are signs that speed equals money in the business aviation market. Ultra-long-range business jet such as Bombardier's Global Express, which typically fly at Ma 0.85, sacrifice range for speed; Cessna's Citation X, for example, is second only to Concorde, with a cruising speed of Ma 0.92. The planes have been surprisingly popular, despite their smaller cabins and limited range.

At present, business jet manufacturers are concentrated in five companies -- Cessna of the US, Bombardier of Canada, Raytheon of the US, Dassault of France and Gulfstream Aerospace Corporation of the US -- together account for 88.2 percent of all business jets in use. [2]

The division of the business jet market

There are roughly nine classes of business jets ranging from simple to complex, with seats from few to many and range from short to far, with unit prices ranging from $2 million to $50 million.

-- Private class: Cessna 510, $2.6 million.

-- Entry class: Cessna's Citation CJ1 and CJ2, $4 million to $5 million each.

-- Light class: Bombardier Learjet 31A, 40, Cessna Citation Bravo, CJ3, Encore. Raytheon's Beechjet are priced between $5 million and $9 million each.

-- Super Light class: Bombardier Learjet 40/45XR, Cessna Excel, $9.5 million - $10 million each.

-- Mid- class: Bombardier Learjet 60, Cessna Sovereign, Gulfstream G-100, G-150, Raytheon Hawker 800XP. The unit price is $11 million to $13 million.

-- Super medium class: Bombardier Challenger 300, Cessna Citation X, Dassault Falcon 50EX, Gulfstream G-200, Raytheon Horizon, etc., each priced between $16 million and $20 million.

-- Big class: Bombardier Challenger 604, 800, Dassault Falcon 2000EX, Gulfstream G-300, $22 million to $27 million each.

-- Supersized class: Bombardier Global Express 5000, Dassault Falcon 900/900EX, Gulfstream G-400/G-500, $30-37 million each.

-- Long-range class: Bombardier Globe Express, Dassault Falcon 7X, Gulfstream G-550. The unit price is between $40 million and $45 million.[3]

Research progresses of SSBJ

In 2010, Lockheed Martin designed an aircraft for NASA called Green Ultrasound, which has a maximum flying Mach number of 2.04. Its upside-down V-shaped engine, like a spoiler on a race car, improves airflow and reduces sonic booms, that was a big feature.

Lockheed Martin's simulations show that the effects of sonic booms in flight have been significantly reduced, and that the aircraft can fly further and use fuel more efficiently. It has an overall canard layout with a slender fuselage to reduce shock drag, large swept trapezoidal wings, and four engines with lower carbon dioxide emissions. The aircraft is sleek and environmentally friendly, hence the name "Green Ultrasound". The project is part of NASA's research into making air travel a reality by 2035, the year it plans to officially use the aircraft for air transport.[4]

Figure 1 – Green Ultrasound

In 1960, Britain and France cooperated in the development of supersonic passenger aircraft - "Concorde" aircraft, it has a maximum flight Mach number of 2.04, a cruising altitude of 18,000 meters, a maximum payload range of 5,110 kilometers, a maximum take-off weight of 186 tons, an empty weight of 78.7 tons, and it can carry 128 passengers, it has a length of 62.1 meters, a wingspan of 25.56 meters, a height of 11.4 meters. Four Rolls-Royce Olympus 593Mk610 turbojet engines provide it with 4 x 140 kN (32,000 lb) of net thrust, starting afterburner :4 * 169 kN (38,050 lb), and the takeoff range is 3,410 m. The landing distance is 2220 meters, take-off noise is 119.5 dB, side noise is 112.2 dB and approach noise are 116.7 dB.

Concorde aircraft generally adopts the canard layout, the wing adopts the delta wing, the leading edge of the wing is S-shaped, the fuselage is slender, and it use the single vertical tail. In order to improve the takeoff and landing field of vision, the nose is designed to adjustable, in the takeoff and landing of a certain Angle, can be lowered 5 to 12 degrees, so that the aircraft in the takeoff and landing, the pilot to obtain excellent field of vision, cruise will turn to normal state. The first Concorde supersonic passenger jet was launched in 1969 and entered commercial flight in 1976. Concorde is the world's only commercial supersonic airliner in service. Only 20 Concordes were ever built. By early 2003, 12 Concordes were still flying commercially. On October 24, 2003, the Concorde made its final flight and was retired altogether because of noise and cost concerns.[5]

Figure 2 – Concorde supersonic jet

An unnamed Japanese supersonic jet, the Japan Aerospace Exploration Agency (JAXA) has had the idea for a supersonic business jet in the works for quite some time, they even tested a small prototype in 2005.

In June 2021, JAXA organized a body called the Japan Supersonic (JSR) Research Council, which included Mitsubishi Heavy Industries, Kawasaki Heavy Industries and Subaru -- all working to build a 50-seater supersonic jet that would consume at least 13% less fuel and have a sonic boom 50% smaller than Concorde.[6]

Figure 3 – An unnamed Japanese supersonic jet

Spike S-512. Spike is a bit of a mystery because it is one of the most successful and prominent supersonic transport projects of the new generation, founded in 2014, Spike tested a small-scale prototype in 2017 and has been in the process of improving it ever since. On the other hand, very little is known about the Spike S-512 project. Except for a few 3D rendering models. As of late 2021, the company hasn't revealed much, or released actual photos.

Spike 's supersonic business jet is envisioned to travel at Mach 1.6, carry 12 to 18 passengers and feature a windowless cabin, an idea that makes engineering easier but has yet to be tested.

Figure 4 – Spike's SSBJ

The one getting the most attention is Boom Technology, which is also one of the leaders in supersonic passenger aircraft. In 2016, the company unveiled the Overture aircraft concept, which has since changed as the company has studied the market.

The Boom concept is much simpler than its rivals: it has a top speed of just Mach 1.7 (2,082 km/h), and the plane lacks any ultra-modern features, such as a windowless cabin and a single-wing design. This means that Overture is only allowed to fly over the ocean, but it can make up for this with cheaper prices and shorter development times.

The company has built a 1/3 scale technology verification aircraft, received a contract from the U.S. Air Force, and has orders from several major airlines. A full-scale prototype of Overture is expected to be tested by 2026 and enter mass production in 2030.

Overture aircraft, the successor to Concorde, even employs former Concorde pilots. Despite the challenges, Boom Technology is the best placed to succeed based on the information that has come to light so far.

Figure 5 – Overture aircraft

Technical characteristics of SSBJ

The supersonic business jet (SSBJ) has been the dream of the aviation industry for decades, and many even think it's inevitable, that it's only a matter of time. Back in the 1960s, NASA studied flying across the Atlantic at speeds of up to Ma 2.7 in a plane carrying 8 to 12 people. Boeing was still working on a 10-seater supersonic jet in 1971, when plans for a 234-passenger Ma 2.7 supersonic transport aircraft were cancelled. In the mid-1970s, NASA worked on an Ma 2.4 business jet, but later opted for a 300-seat high-speed civilian transport aircraft (HSCT). The project was cancelled in 1999 when Boeing lost interest. Recently, countries are developing supersonic transport aircraft.

The obstacles to developing a commercial supersonic transport aircraft are thought to be easier to overcome if they are made small, since things like noise emissions and sonic booms are directly related to the weight of the aircraft. But business jet manufacturers don't have the resources to develop the vast array of technologies needed to make supersonic jets, no matter how developed their market becomes. So, while SSBJ continue to work at a low level, many companies are waiting for a breakthrough elsewhere in the aviation world.

These breakthroughs are unlikely to come soon from the commercial air sector, as airlines now go for low costs and efficiency rather than high speeds and fares. But there is hope for the military, especially as the United States increasingly focuses on high-speed,

long-range attack aircraft. The lightweight construction and long-life engine developed by the Pentagon could combine with NASA-funded research into low-boom layouts and low-emission powerplants to create the conditions for a supersonic business jet within the next decade.

A key factor in the success of supersonic business jets may be "partial ownership," which lowers the barriers to purchase and allows more people to enter the market to enjoy such expensive planes. "Part-owned" operator Net Jet's experience with Citation X shows that the fruit is shared, and the speed is popular.

Gulfstream has made more than one attempt at a supersonic business jet, working with the Sukhoi Design Bureau in the early 1990s to develop the Ma 2 SSBJ with a range of 7,500km, but to no avail. In the late 1990s, Gulfstream teamed up with Lockheed Martin's Weasel Works to win U.S. government funding for a demonstration of low-noise supersonic aircraft technology. The collaboration was short-lived, but it helped spawn the Defense Advanced Research Projects Agency's Quiet Supersonic Platform (QSP) program. The goal of the program is to validate the technology needed for long range strike aircraft and SSBJ.

Since Concorde's maiden flight, airport noise and sonic booms have plagued supersonic transport aircraft. Reducing the cruising speed below Ma2.0 without afterburner will help the SSBJ's success, but noise is directly related to thrust, so reducing the weight of the aircraft will be crucial.

Reducing weight is also crucial to reducing sonic booms. There is no formal definition of what constitutes an "acceptable" sonic boom, but work on NASA's High Speed Civilian Transport Aircraft (HSCT) program suggests that overpressure on the ground of no more than 0.3 pounds per square inch may be considered low enough to allow unrestricted supersonic travel over land. The strength of the sonic boom is proportional to the weight of the aircraft, so smaller business jets have an advantage over larger transport aircraft. Further changes in sonic boom characteristics may also reduce overpressure.

One of the main indicators of the QSP program is that, to prove in flight, sonic booms can be reduced by changing the shape of the aircraft, such as a rounded, blunt nose, slender fuselage, long-stringed wings and other measures known to reduce overpressure near the aircraft.

Dassault's approach to overcoming airport noise and sonic booms is to add more

engines for efficient and reliable sustained supersonic cruise flight. The turbine inlet of a subsonic airliner engine is only allowed to reach its maximum temperature within three minutes of takeoff; Fighters are only allowed five minutes to reach maximum temperature during operations. But supersonic business jets must be kept in hot conditions for several hours, with 2,000 hours between refills. None of today's engines can do that.

An engine capable of sustained supersonic cruise flight must have large main culverts. Dassault estimates that its supersonic Falcon's three engines (each with 12,000 pounds of thrust) have the same main culvert size as a subsonic engine producing 40,000 pounds of thrust. Dassault says SSBJ engines may need variable cycles during takeoff and landing. In the other words, take off and land at a high bypass ratio to reduce noise, and cruise over long distances at a low bypass ratio to reduce drag.

Conclusion: Supersonic cruise capability refers to the ability of aircraft to carry out supersonic flight continuously in the case that the engine does not turn on afterpressure. The supersonic cruising aircraft can reach the destination in a short time at the supersonic degree, which is impossible for subsonic aircraft to complete the task, which is the biggest advantage of supersonic cruising aircraft. However, the supersonic cruise aircraft still has some shortcomings, mainly as follows:

(1) Due to the existence of shock drag during supersonic cruise, the lift-drag ratio K decreases significantly compared with subsonic cruise.

(2) It is difficult to meet environmental standards in supersonic cruise condition with large oil consumption, serious waste gas pollution, large aerodynamic noise and strong sonic boom when passing the sound barrier.

(3) The measures adopted in favor of supersonic cruise make the low speed performance of take-off and landing state poor.

(4) For large supersonic cruise transport aircraft, the structural strength of materials is required to be higher.

(5) For the transport aircraft with high cruising Mach number, it is difficult to keep aerodynamic heat protection and pressure stable in the cabin.

Main work of this paper

The main purpose of this paper is to design a supersonic business jet with superior

aerodynamic characteristics and beautiful appearance, which is suitable for long-distance business flights. The main contents of this paper are as follows:

1. The design part, according to the proposed design requirements, the overall design of supersonic business aircraft is completed. These include the design of the fuselage segment, the selection of the airfoil, the design of the wing, the selection and layout of the engine, the design of the landing gear, the aerodynamic layout of the aircraft.

2. The establishment of 3D model. Firstly, the basic theory of computational fluid dynamics is introduced, according to the aircraft data designed above, Siemens NX software was used to build the 3D model of the designed aircraft, and Gambit software was used for grid division. To prepare for the simulation analysis with FLUENT software in the next stage.

3. In the third part, FLUENT software is used to calculate the aerodynamic characteristics of each flight state of the designed supersonic business aircraft, and the calculation results are analyzed in detail. These include take-off and landing conditions, high subsonic flight conditions, supersonic cruise conditions.

4. The fourth part summarizes the research work done in this paper, expounds the work completed in this paper and analyzes the existing deficiencies, and looks forward to the content of further research on this subject in the future.

1 Design Section

1.1 Design requirement

This paper mainly studies supersonic business jets. According to some parameters of existing supersonic fighter, the weight, size, range and other performance requirements are determined, as shown in Table 1.1.2:

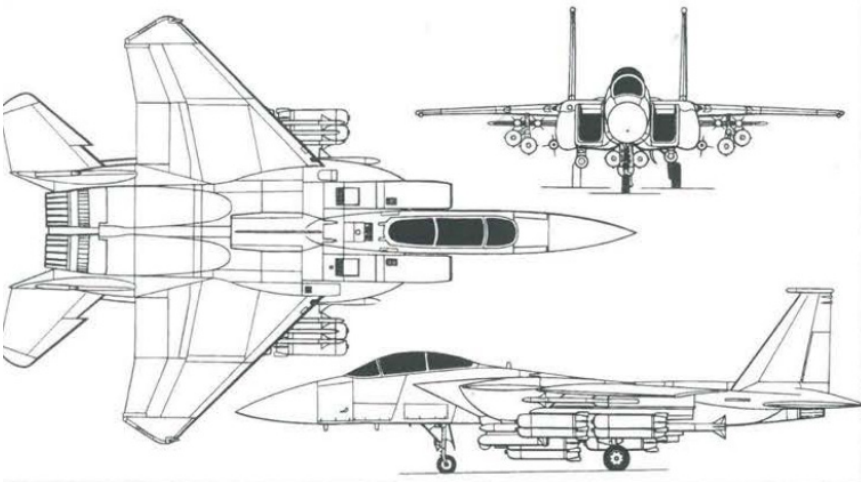

Figure 1.1.1 – F-15

F-15 Eagle is an all-weather, highly maneuverable tactical Fighter aircraft designed to achieve and maintain air superiority. It is one of the main fighter aircraft in service of the United States Air Force. F-15 is developed from the F-X(Fighter-experimental) program launched in 1962. It was won by McDonnell Douglas in 1969, first flew in July 1972, and the first production aircraft was delivered to the U.S. Air Force in 1974, where it has been since.

Figure 1.1.2 – F-22

F-22 Raptor is a heavy stealth fighter jointly designed for the United States Air Force by Lockheed Martin, Boeing, General Dynamics and other companies. Its technical performance is extremely advanced. In the early 21st century, F-22 Raptor is the world's most advanced fighter jet. A comparable fighter jet is estimated to be at least 20 years away. The F-22 has several characteristics across the ages:

Low detectability (stealth ability)

Supersonic cruise (no afterburner, supersonic endurance for a long time)

Highly complex integrated electronic control system (with good control ability and excellent mobility performance)

Figure 1.1.3 – Su-35

Su-35 is a multi-role fighter aircraft produced by the Russian Sukhoi Company with a single seat, twin engines and double vertical tail. It has long range, multi-purpose, air superiority and strike characteristics. Belongs to the 4.5th generation heavy fighter (using 5th generation technology on 4th generation aircraft)

Figure 1.1.4 – EF-2000

EF-2000 (Typhoon) is a new single-seat dual-engine supersonic fighter developed by Eurofighter (a collaboration between Britain, Germany, Italy and Spain). It is a predecessor of the EFA validation aircraft, formerly named EF2000. The aircraft is mainly used for air defense and air superiority missions, with both ground attack capabilities.

Typhoon fighter adopts the layout of pre-duck-type delta wing, double engine, single vertical tail and belly inlet. It is a multi-purpose air superiority fighter with over-the-horizon, aerial super maneuvering attack and combat capabilities, as well as short takeoff and landing (STOL) capability, "supersonic cruise" capability and certain ground attack capability. Sustained flight above the speed of sound without the use of afterburner.

Table 1.1.1 – Statistics prototype aircraft

	Airplane	F- 15	F-22	Su-35	EF–2000
Flight data	V_{max}, Mach	2.5	2.25	2.25	2
	H_{max}, km	20	19.8	18	19
	V_{cr}, Mach	1.2	1.5	1.5	1.2
	H_{cr}, km	17	13	16	16
	L (m_{tmax}), km	5700	5700	4600	3900
	L (m_{CARmax}), km	5445	5500	4500	3800
	L_{land}, m	-	900	300	700
	$L_{take-off}$, m	-	915	300	700
Weight data	m_{empty}, t	14.5	19.6	18.4	11
	$m_{0\,max}$, t	36.7	37.6	34.5	23.5
	N_{pas}, people	1	1	1	1
	m_f, t	6.0	8	5	4.5
Power	Type of engine	turbofan	turbofan	turbofan	turbofan
	Number of engines	2	2	2	2
	P_0, kN	110	158	142	91
Geometric data	S, m^2	56.49	78	62	51.2
	l, m	13.05	13,56	15.3	11
	χ	45	42	53	53
	λ	3.0	2.36	2.5	2.6
	η	5	6	5	6
	L_f, m	19.43	19	21.9	16
	D_f, m	2	2	2	2
	λ_f	10	9.5	11	8
	S_{GT}, m^2	10.34	12.63	-	-
	χ_{GT}	50	-	-	-
	S_{VT}, m^2	9.78	16.54	-	-
	χ_{VT}	37	-	-	-

Table 1.1.2 – Tactical-technical requirements of model SSBJ

Parameters	Full name	Value
$\boldsymbol{R}$	Lifetime， hours	60000
$\boldsymbol{V_{cr}}$	Cruising speed, M_a	1.7
$\boldsymbol{V_{max}}$	Maximum speed, M_a	1.8
$\boldsymbol{L}$	Flight range, km	6000
$\boldsymbol{L_{take-off}}$	Take-off run length, m	2100
$\boldsymbol{N_{pas}}$	Number of passengers	10
$\boldsymbol{H_{cr}}$	Cruise flight altitude, Km	30

According to statistical data, the main parameters of the wing, the fuselage are determined and recorded in table 1.1.3.

Table 1.1.3 – Main aircraft parameters

Parameters	Full name	Value
$\boldsymbol{\eta}$	Wing taper	3.1
$\boldsymbol{\lambda}$	Wing aspect ratio	4
$\boldsymbol{\chi}$	Wing sweep angle	42
$\boldsymbol{\lambda_{VT}}$	Vertical tail aspect ratio	2
$\boldsymbol{\lambda_{GT}}$	Horizontal tail aspect ratio	4
$\boldsymbol{\eta_{GT}}$	Horizontal tail wing taper	4
$\boldsymbol{\eta_{VT}}$	Vertical tail wing taper	3
$\boldsymbol{\chi_{GT}}$	Horizontal tail sweep angle	22
$\boldsymbol{\chi_{VT}}$	Vertical tail sweep angle	33
$\boldsymbol{\lambda_f}$	Fuselage aspect ratio	10.8
$\boldsymbol{D_f}$	Fuselage diameter	3.7

On the basis of statistical data processing, an unconventional aerodynamic configuration was selected for the model aircraft, which was canard layout and swept back delta wing structure. Adopt pencil type slender body, engine at the tail, tricycle landing gear with nose wheel, which has minimal noise pollution during supersonic cruise. The internal structure of the fuselage, cabin and cargo hold is simplified.

Such a design has several advantages:

--- Delta wing is characterized by high critical point of stall, faster flight speed, and can effectively reduce the problem of ultra-highly speed jitter.

--- The delta wing layout has a large sweep Angle, which not only reduces the shock wave intensity of the leading edge of the wing, but also makes the position of the shock wave spread along the axis of the aircraft, so as to avoid the shock wave system gathering in the same station. At the same time, the distribution law of the supersonic area of the aircraft with large swept delta wing layout is generally relatively uniform, which avoids the sudden increase of the cross the section area, and also helps to reduce the intensity of sonic explosion.

--- The slender front fuselage of the aircraft can not only obtain higher low-speed elevation Angle lift, which is conducive to takeoff and landing, but also reduce the drag generated during supersonic flight, which is conducive to supersonic flight.

--- The canard layout improves the total lift of the aircraft. The canard wings in front of the main wing can generate part of the lift force. Meanwhile, after the air flow flows through the canard wings, eddy currents are generated on the upper surface of the main wing, which increases the pressure difference between the upper and lower surfaces of the main wing and forms lift increment on the original basis, which increases the total lift force and improves the lift characteristics of the canard layout aircraft.

--- Tricycle landing gear with nose wheel provides a more effective braking when run, substantially reducing the possibility of bouncing，improve visibility during takeoff - landing pilots. In addition, the circuit with the chassis nose wheel has better stability when driving on the airfield.

--- The advantage of having the engine aft：

1. There is no excess bulge under the wing, reducing the impact of the engine pod on

lift and drag;

2. There is no requirement for the space under the wing, so the designer can shorten the height of the landing gear and save the weight of the structure;

3. It can provide a quieter and more comfortable environment for the first class, business class and even high-end economy class at the front of the fuselage;

4. Due to the close distance between the two engines, once the single engine fails, the impact on the yaw of the aircraft is far less than that of the underwing hanging layout.

Along with the advantages of this scheme has the following disadvantages:

--- The canard layout reduces the stability of the aircraft. Aircraft maneuverability and stability are contradictory, good stability is bad maneuverability, and vice versa. For the canard wing layout, the aircraft is statically unstable, and the canard wing deflection needs to be constantly adjusted according to the flight state of the aircraft to maintain the balance of the aircraft, and the stability of the aircraft is suppressed

--- Large Angle swept wings can cause wing tip stall problems. Because of the constant flow of air towards the wing tip, the wing tip boundary layer builds up so thick that it can easily stall. The left and right tips are unlikely to stall at the same time, so either stall first causes the plane to roll and sway, and because the wingtips extend backwards, the wingtip stall also causes the plane to pitch.

--- The maximum lift coefficient of delta wing is small, so it is difficult to land. Because the delta wingspan aspect ratio is small, so the glide performance is poor, when the engine is not working is a big problem.

--- Since the engine is mounted at the tail, the intake is inefficient and inconvenient to repair. And the rear-mounted engines are heavy, making trim a challenge.

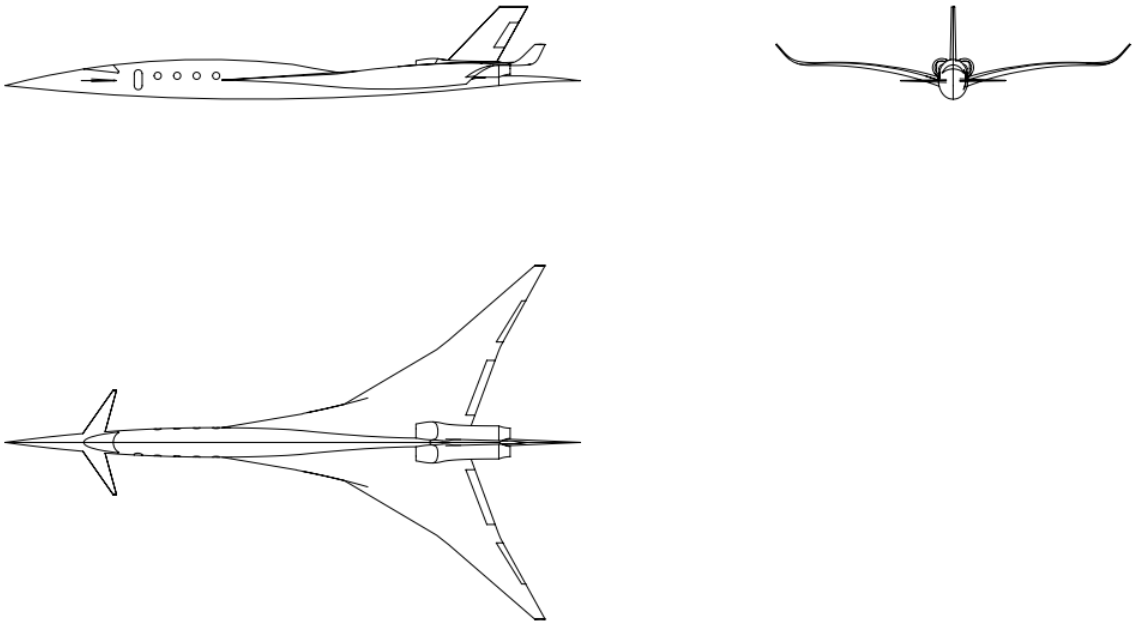

Figure 1.1.5 – scheme of model SSBJ

1.2 Main parameters estimation

1.2.1 Calculation of the aircraft takeoff mass in three approximations.

1.2.1.1 Determination of take-off weight of the aircraft in zero approximation

Determination $\mathbf{m_0}$ is available in several approximations updating via relative masses mi obtained by examining statistics of prototypes and comparative analysis of aircraft.[10]

Take-off weight in the zero approximation, given by:

$$m_0^0 = \frac{m_C + m_{CR}}{1 - (\bar{m}_k + \bar{m}_{pp} + \bar{m}_{EQ} + \bar{m}_F)}. \quad (1.1)$$

Where m_0^0 – take-off mass of the airplane in zero approximation; m_C – mass of cargo (payload); m_{CR}– mass of crew; mass ratio of the airplane structure. $\bar{m}_F$ – mass ratio of fuel. According to the list of empirical coefficients, let $\bar{m}_k = 0.24$; mass ratio of power-plant $\bar{m}_{pp} = 0.10$; mass ratio of equipment $\bar{m}_{EQ} = 0.07$.

Operating mass:

$$m_{CR} = 80\, n_{CR} + \triangle\, m_{CR} = 80 * 2 + 120 = 280 \text{ kg};$$

m_C payload weight = + m_{PAS}+ Business decoration load:

$$m_C = 90\, n_{PAS} + \triangle\, m_C = 90 * 10 + 4820 = 5720 \text{ kg};$$

Relative fuel mass

$$\bar{m}_F = a + \frac{bL}{V}. \tag{1.2}$$

L – Flight range, L = 6,000 km;

V – Average cruising speed, V = 2000 km/ h;

a = 0.05; b = 0.13.

Then

$$\bar{m}_F = 0.05 + \frac{0.13 * 6000}{2000} = 0.44.$$

Substituting the values of the relative masses and predetermined in dependence define takeoff weight in zero approximation:

$$m_0^0 = \frac{5720 + 280}{1 - (0.24 + 0.10 + 0.07 + 0.44)} = 40000\text{kg}$$

Define the airframe weight: $m_k = \bar{m}_k * m_0^0 = 0.24 * 40000 = 9600\text{kg}$

Power plant weight: $m_{pp} = \bar{m}_{pp} * m_0^0 = 0.1 * 40000 = 4000\text{kg}$

Equipment mass: $m_{EQ} = \bar{m}_{EQ} * m_0^0 = 0.07 * 40000 = 2800\text{kg}$

Fuel mass: $m_F = \bar{m}_F * m_0^0 = 0.44 * 40000 = 17600\text{kg}$

Table 1.2.1: The value obtained by calculating the mass

m_0, kg	m_k, kg	m_{pp}, kg	m_{EQ}, kg	m_F, kg
40000	9600	4000	2800	17600

1.2.1.2 Determination of take-off weight of the aircraft as a first approximation

The main difference between this calculation by calculation m_0^0 is taken into account,

depending the takeoff weight of the aircraft, the wing parameters and other parts of the aircraft, the flight mode. Due to the fact that $\bar{m}_c$ very difficult to depend on the take-off weight, it is necessary to calculate the m_0^1use either a graphical method of solving the equations of mass balance of the aircraft, or successively closer to the solution and find it with the help of computers. Input data are given in table 2.1.2.

(1). Influence of parameters on the wing lift coefficient in the separation and quality of the separation:

As studied parameters, choose elongation wing and its angle of sweep. The coefficient of lift during takeoff determined by the formula:

$$C_y = C_{y_{cr}}^{iso}\left(1 + \Delta\overline{c_y}\frac{\delta_{fd}}{\delta_{tfd}} \cdot \overline{S_{mec}^{lSO}} \cdot COS^2\chi_{0.75}\right) + \Delta\overline{c_{gr}} + \Delta\overline{c_{ybl}}. \quad (1.3)$$

Where: $C_{y_{cr}}^{iso}$- lift coefficient of the wing when without isolation mechanization:

$$C_{y_{cr}}^{iso} = C_y^{\alpha} \cdot \alpha_{iso}. \quad (1.4)$$

C_y^{α} – lift coefficient derivation angle of attack, 1/deg:

$$C_y^{\alpha} = \frac{0.11 - 0.029\sqrt[4]{\bar{c}}}{\frac{0.775}{cos\chi_{0.5}} + \frac{1.5}{\lambda}}. \quad (1.5)$$

Where: $\bar{c}$- the relative thickness of the profile;

$\chi_{0.5}$ – sweep angle of the wing chord of 50%;

λ – wing aspect ratio;

$\Delta\overline{c_y}$ – Increased lift coefficient by using adjustable flap;

δ_{fd} – flap deflection angle during takeoff, deg;

δ_{tfd}- flap deflection angle;

$\overline{b_3}$- Relative to the chord of the flap;

b_{3table}- Relative flap chord;

S_{mec}^{iso} – The relative area of the console serviced by mechanization;

$\chi_{0.7}$ – Sweep 0.75 chords in the area of mechanization;

$\Delta\overline{c_{gr}}$ – Increase in the lift coefficient due to the ground effect;

$\Delta\overline{c_{ybl}}$ – Increased lift coefficient due to blowing wing screws;[11]

Increased lift due to the ground effect can be estimated by the formula:

$$\Delta C_{y_{gr}} = 0.313 - 0.237\bar{h} + 0.0572\left(\bar{h}\right)^2. \quad (1.6)$$

Table 1.2.2: Effect on elongation wing lift coefficient in the separation

λ	2	4	6	8	10	12	14	16	18	20	22
C_y	0.87	1.17	1.27	1.33	1.36	1.38	1.4	1.41	1.42	1.43	1.43

Table 1.2.3: Effect of wing sweep on lift coefficient in the separation

λ	0	8	16	24	32	40	48	56	64	72	80
χ	1.4	1.42	1.39	1.33	1.22	1.09	0.93	0.76	0.6	0.46	0.32

(2). Investigation of the influence parameters on the plane of required starting thrust-administrative supersonic aircraft turbojet

As studied parameters, choose elongation wing and its angle of sweep.

The following relationships are used to study the influence of parameters on the thrust-weight ratio, the need for cruise t_{0cr}:

$$t_{0cr} = \frac{0.953 p_n M_{cr}^2}{\xi_{cr}}\left(\frac{F_1}{p} + F_2\right). \quad (1.7)$$

Where p_n- atmospheric pressure at cruising altitude, daN/m^2;

$\xi_{cr} = \xi_v \xi_H \xi_{al}$- coefficients taking into account the change in engine thrust for speed ξ_v and altitude ξ_H, Thrust reduction due to losses in the dunamic pressure air intakes ξ_{taken}, Engine operation $\xi_{et\ al}$.

$$\xi_v = 1 - (0.5 + 0.133y - 0.0069y^2)M + (0.6 + 0.01y)M^2; \quad (1.8)$$

$$\xi_H = \frac{P_H}{P_0}(\frac{T_0}{T_H})^{2+0.2y}. \quad (1.9)$$

Coefficient of frontal drag of the wing is calculated using the formula:

$$F_1 = k_0(C_{xcr} + C_{xw.cr}). \quad (1.10)$$

Where in drag coefficients C_{xcr} and wave drag $C_{xw.cr}$ for a wing determined by the relationships:

$$C_{x\,trcr} = \frac{0.174(1+2\bar{c}+9\bar{c}^2)(1+2\bar{c}M_{cr})}{(lg-1.6)^2\sqrt{1+0.2M_{cr}}}\left(1 - k_{int}\overline{S_f}\right) + 0.001\bar{\rho}_{sch}; \quad (1.11)$$

$$Re_{cr} = f(H) \cdot M_{cr}\sqrt{\frac{g \cdot m_{pl}}{10\lambda k_0 p}}; \quad (1.12)$$

$$f(H) = [2.33\left(1 - \frac{H}{12} + 0.0045H^2\right] \cdot 10^2; \quad (1.13)$$

$$C_{X\,wave.cr} = C_{X\,W.max}\left(\frac{M_{cr} - M_{crit.cr}}{M_{cx.b.max} - M_{crit.cr}}\right)^3 \cdot \left(4 - 3\frac{M_{cr} - M_{crit.cr}}{M_{cx.b.max} - M_{crit.cr}}\right); \quad (1.14)$$

$$C_{X\,B.max} = \frac{2\pi\lambda(\bar{c})^2 cos^2\chi_{0.5}}{2 + \lambda(\bar{c})^{1/3}cos^{5/3}\chi_{0.5}}; \quad (1.15)$$

$$M_{cx\,B.max} = \frac{1}{cos\chi_{0.5}}\left[1 + 0.4\frac{\bar{c}^{\frac{2}{3}}}{cos^{\frac{2}{3}}\chi_{0.5}}\left(2 - \lambda(\bar{c})^{\frac{1}{3}}cos^{\frac{2}{3}}\chi_{0.5}\right)\right]; \quad (1.16)$$

$$M_{crit.cr} = 1 - \frac{0.7\lambda^2\sqrt{\bar{c}}}{\lambda^2 + 0.1}cos\chi_{0.5}; \quad (1.17)$$

Coefficient of frontal drag fuselage and nacelles determined by the expression:

$$F_2 = \frac{(C_{xf}+C_{x\,wave.f})}{k_{mid}}. \quad (1.18)$$

Where in drag coefficients C_{xf} and wave drag $C_{x\,wave.f}$ defined by the relationships:

$$C_{x\,tr.f} = 3.1\lambda_f(1+0.1M_{cr}^2)^{-0.67}\left[\frac{0.455}{(lgRe_f)^{2.58}} - \frac{1700}{Re_f}\right]; \quad (1.19)$$

$$Re_f = f(H)M_{cr}\lambda_f d_f;\ C_{x\,wave.f} = \frac{1}{4\lambda_p^2+1}. \quad (1.20)$$

$$\text{If a} M_{cr} \geq 1 - \frac{1}{\lambda_f+2\lambda_p}. \quad (1.21)$$

To investigate the effect of geometrical parameters of the wing and its thrust-to mechanization needs to provide a predetermined length of start before take-off, the following relationship is used:

$$t_{0to} = \frac{1}{\xi_{fl}}\left[\frac{0.832p}{C_y \cdot L_{land}} + \frac{1}{3}\left(\frac{1}{K_{sep}} + 2f\right)\right]. \quad (1.22)$$

The magnitude of the starting thrust-weight ratio, need to ensure a predetermined climb gradient in accordance with airworthiness aircraft (CONCORD), defined by the formula:

$$t_{0wit} = \frac{n_{en}}{\xi_{fl}(n_{en}-1)}\left(\frac{1}{K_{sep}} + tg\theta\right). \quad (1.23)$$

The value of tg0 set in CONCORD.

(3). Calculation of the relative weight of the wing:

To calculate the relative weight of the wing formula is used:

$$\bar{m}_{cr} = \frac{7.2k_1 n_A^p m_0^{0.5}\phi\lambda}{10^4 p\bar{c}^{0.5}{}_0 cos^{1.5}\chi_{0.5}} \cdot \frac{\eta+4}{\eta+1} \cdot \frac{4.5k_2k_3}{p} + 0.015\,. \quad (1.24)$$

Where:

k_2 - coefficient reflecting type panels;

k_2- coefficient that takes into account the presence of sagging wing spoilers, slats;

k3 - coefficient; method which takes into account wing seal for containing fuel.

G- factor n_A^p:

$$n_A^p = n_{op} \cdot 1.5$$

$$n_{op} = 2.1 + \frac{10890}{m_0+4540} = 235; f = 1.5;\ as\ n_{op} < 2.5 \quad \text{we accept } n_{op} = 2.5;$$

$$n_A^p = 2.5 \cdot 1.5 = 3.75;$$

$m_0 = \frac{m_0}{k_{otd}}$ – the value of the take-off weight of the aircraft-approaching zero;

$\varphi = b - 0.83\bar{m}_f$ – discharging wing fuel ratio and the engine;

P – Specific load on the wing, daN/m^2

$\lambda, \bar{c}, \chi_{0.25}, \eta$ – aspect ratio, relative thickness of the profile at 1/4 wing chord sweep angle.

(4). Calculations of the relative weight of the fuselage:

Relative fuselage mass is determined by the formula Schein.

$$\bar{m}_f = k_1 \cdot \lambda_f \cdot d_{cr}^2 \cdot (\frac{m_{com}}{k_{otd}})^i + k_2 + k_3 + k_4\,. \qquad (1.25)$$

Where:

k_1=3.63…0.333d_f;

$i = -0.743$

k_2 - Coefficient taking into account the place of fastening the main landing gear;

k_3- Coefficient reflecting spot cleaning main landing gear;

k_4 - Coefficient accounting method for loading luggage.

(5). Calculation of the relative mass of tail

Relative weight tail is determined by the statistical formula:

$$\bar{m}_{wt} = 0.85 \cdot k_p \cdot k_{wt}^{cx} \cdot p^{-0.56} \cdot \bar{S}_{wt}^{1.16} \cdot (\frac{m_{com}}{k_{otd}})^{0.16}\,. \qquad (1.26)$$

Where: k_n=1 at $p \le 450 daN/m^2$;

$$\bar{S}_t = \bar{S}_{g.t} + \bar{S}_{v.t}\,. \tag{1.27}$$

$$k_t^{cx} = \frac{1.333 - 0.0011 \cdot S_t}{1.295 + 0.0028 \cdot p} \tag{1.28}$$

$$S_{t.} = S_t \frac{m_{pl}}{p \cdot k_{otd}} \tag{1.29}$$

Table 1.2.4: Effect of the specific load on the weight empennage

P, daN/m^2	100	200	300	400	500	600	700	800	900
$\bar{m}_t$	10.0931	0.0653	0.0497	0.037	0.025	0.0207	0.0175	0.015	0.0131

(6). Calculation of the relative weight of the landing gear:

The relative weight of the landing gear is determined by the formula Fadeyeva.

$$\bar{m}_{lg} = k_{lg} \cdot k_{fd} \cdot \frac{\frac{m_{com}}{k_{otd}} + 20400}{\frac{m_{com}}{k_{otd}} + 79000}\,. \tag{1.30}$$

Where: k_{fd}= 0.02728- coefficient taking into account the influence of the fuselage diameter and type of engines on the weight of the chassis;

k_{lg}= 1 -coefficient reflecting the number of main landing gear;

$$\bar{m}_{lg} = 1 \cdot 0.02728 \cdot \frac{\frac{9600}{0.212} + 20400}{\frac{9600}{0.212} + 79000} = 0.067\,.$$

Thus, the above formula allows analyzing separately depending on the relative masses of the wing, tail, fuselage, landing gear and large dependence of the relative weight of the airframe on the specific load on the wing, the takeoff weight of the aircraft airframe and geometrical characteristics.

(7). Calculation of the relative weight of the power plant:

The relative mass of the power plant is determined by the formula:

$$\bar{m}_{pp} = R \cdot \gamma_{en} \cdot t_{0\,max}\,. \tag{1.31}$$

Where: R - coefficient taking into account the increase in mass of the power plant compared to the mass of engines;

$$R = k_1\left(1 + 0.1\frac{n_{en.r}}{n_{en}}\right) \cdot \left[1 + \frac{0.0236}{\gamma_{en}} \cdot (1.5 + 0.275 \cdot y^{0.75})^2\right]. \tag{1.32}$$

Where: k_1- Coefficient taking into account the number and location of the engine.

n_{en}-The number of engines installed on the aircraft;

n_{enr}-Number of engines equipped with thrust reversers;

γ_{en}-Specific weight of the engine;

y - Degree of engine bypass.

(8). Calculation of the relative weight of fuel:

The relative fuel mass is the sum:

$$\bar{m}_f = \bar{m}_{fcc} + \bar{m}_{fcf} + \bar{m}_{fcr} + \bar{m}_{fns} + \bar{m}_{fuc}. \tag{1.33}$$

Where: $\bar{m}_{fcc}$ - relative weight of fuel consumed in the climb;

$\bar{m}_{fcf}$ - relative fuel mass consumed for lowering and landing;

$\bar{m}_{fcr}$- relative weight of fuel consumed in cruising flight;

$\bar{m}_{fns}$ - relative weight navigational fuel supply;

$\bar{m}_{fuc}$= 0.006 - relative weight of unaccounted fuel consumption (No residue produced);

$$\bar{m}_{fcc} = \frac{0.0035 \cdot H_{fir}(1 - 0.03y)}{1 - 0.04 \cdot H_{fir}} \tag{1.34}$$

Where: H_{fir}, H_{end}- initial and final cruising altitude;

y- bypass ratio engine

The relative fuel mass for cruising flight navigation margin determined by the formula:

$$\bar{m}_{fcr} + \bar{m}_{fns} = 0.052 + \left[\frac{0.2(L - 40H_{sr})}{a_H M_{cr} - 0.28W_a} + 1\right] \cdot C_{p.cr}\sqrt{\frac{k_2(1+\overline{S_f})}{k_1 \cdot \lambda}}(F_1 + F_2 P) \tag{1.36}$$

$$H_{sr} = \frac{(H_{fir} + H_{end})}{2} \tag{1.37}$$

Where: L- range in km;

a_H- speed of sound at the average cruising altitude m/s;

M_{cr}- Mach number corresponding to the cruising speed;

W_β- Headwind km/h;

$C_{p.cr}$- Specific fuel consumption at cruising flight. $Km/h\ daN$.

Expression $k_2\left(1+\bar{S_f}\right)/k_1 \cdot \lambda$ represents a ratio of blade polar. Where k_1 accounts for the effect of sweep. But k_2 effect elongation of the wing;

Where: $\chi_{0.25}$ – Sweep 1/4 chord hail;

k_2=1.02- for λ< 4.5

Specific fuel consumption is determined by the formula:

$$C_{p.cr} = \frac{0.85}{1+0.37y^{0.75}}\left[1+(0.27+0.2y \cdot M_{cr}^2)\sqrt{M_{cr}} - 0.02H_{sr}\right] \tag{1.38}$$

(9). Calculation of the relative weight of the crew, equipment and payload

Crew weight is determined by its number, which depends on the type of aircraft. The mass of a crew member is 80 kg. In this way:

$$m_{cr} = 80 \cdot n_{cr} \tag{1.39}$$

Where: n_{cr} - the number of crew members, including flight attendant;

Weight of the equipment, measured in kilograms.

$$m_{eq} = 95 \cdot n_{pas} \cdot (5 \cdot 10^{-5} \cdot L_{mec} + 0.66) \tag{1.40}$$

Technical determined distance in kilometers:

$$L_{mec} = L + 700 \tag{1.41}$$

L= 3000 - the range of the airplane with a specified number of passenger kilometers.

$$L_{max} = 6000 + 700 = 6700$$

$$m_{eq} = 95 \cdot 10(5 \cdot 10^{-5} \cdot 6700 + 0.66) = 945$$

Mass of payload, $m_{com} = 5700kg$

The total weight, kg.

$$m_{sum} = m_{op} + m_{com} + m_{eq} = 7345\ kg$$

1.2.1.3 Calculation of the mass of the aircraft in the second approximation

Calculation of mass of the aircraft in the second approximation provides clarification weight aircraft structure – individual units using analytical formulas.[10]

Supersonic wing aircraft is calculated by the formula:

$$m_w = 1.14 \cdot 10^{-4} k_{mec} k_{con} k_{n.m} \varphi_2 n_p \cdot \frac{\lambda}{cos^{1.5}{}_{\chi_{0.25}}} \sqrt{\frac{(m_0')}{p\theta \bar{c}_0}} \cdot \frac{\eta + 4}{\eta + 1} (1 - \frac{\mu - 1}{\eta + 3}) \quad (1.42)$$

Where m_0' - the mass of the aircraft, resulting in first approximation, m_0'=39.25t;

k_{mec} - Mechanization coefficient k_{mec}= 1.4;

k_{con}= 0.9;

b= 0.87- Aircraft with the engines on the tail;

$\theta = 0.9$, for two-spar of the wing;

$\mu = 1.8$, the ratio of relative thicknesses at the root and at the end respectively.

Fuselage mass is calculated by the formula:

$$m_{fus} = 0.003\lambda_f m_0' + 10 d_f^2 \lambda_f + 8 d_f^3 + 150M + 300 + 0.03 k_f m_0' \quad (1.43)$$

Where λ_f=10.8– elongation fuselage;

$d_f = 3.7$ – diameter of the fuselage;

M = 1.7 – design Mach number;

$k_f = 1$, as the main landing gear mounted on the fuselage and removed it;

$$m_{fus} = 0.003 \cdot 10.8 \cdot 39250 + 10 \cdot 3.7^2 \cdot 10.8 + 8 \cdot 3.7^2$$
$$= 150 \cdot 1.7 + 300 + 0.03 \cdot 39250 = 3950\ kg$$

Tail mass calculated by the formula:

$$m_{tail} = (0.946 + 1.5 \cdot 10^{-3} v_{cr})(4.4 + 8 \cdot 10^{-4} m_0')(\bar{S}_{GT} + \bar{S}_{VT}) \frac{m_0'}{P} \quad (1.44)$$

Where $v_{cr} = 2000 km/h$, the calculated airspeed;

$$m_{tail} = 2897\ kg$$

Landing gear mass is calculated by the formula:

$$m_{lg} = 0.032 m_0' \frac{m_0' \cdot 10^{-3} + 359}{m_0' \cdot 10^{-3} + 249} = 1735\ kg \quad (1.45)$$

Equipment and management of mass is calculated as follows:

$$m_{eq} = m_{p.0} + 0.05 m_0' + (1 + 2.7 \cdot 10^{-4} \cdot M^6)(30 n_{cr} + 0.02 m_0') \quad (1.46)$$

Where $m_{p.0} = 560$, Mass radio equipment;

$$m_{eq} = 3460\ kg$$

Aircraft weight in the second approximation is given by:

$$m_0'' = \frac{m_{pl} + m_{op} + m_{eq} + m_w + m_{fus} + m_{tail} + m_{lg}}{1 - (\bar{m}_{pp} + \bar{m}_f)} \quad (1.47)$$

$$m_0'' = \frac{9600 + 700 + 3460 + 3698 + 3948 + 2897 + 1735}{1 - (0.14 + 0.21)} = 40000\ kg$$

1.2.2 Wing load

The value of wing load is obtained by dividing the weight of the aircraft by the wing area of the aircraft. Like thrust-to-weight ratio, wing-load generally refers to the wing-load of an aircraft during takeoff, but can also refer to wing-load under other flight conditions. Wing load affects climb rate, stall speed, takeoff and landing distance, and hover performance. The wing load determines the design lift coefficient and affects the wetted area and wingspan, thus the drag. Wing load greatly affects the takeoff weight of an aircraft. To reduce wing load, you need to increase the wing size. This improves aircraft performance, but adding wings leads to additional drag and empty weight, resulting in an

increase in total take-off weight.[12]

Representative wing loads are given in the table below. These parameters can provide reference in the design process, and can also be used to test the design results.

Table 1.2.5: Typical takeoff wing load statistics

Aircraft type	Value (9.8 N/m ²)
Jet trainer	244
Jet fighter	342
Jet transport / bomber aircraft	586

The aircraft designed in this paper is a supersonic passenger jet, so it can take a large wing load. Combined with the design characteristics of this machine, the wing load of this machine is preliminarily selected to be about 5700 N/m ².

1.2.3 Aircraft lift-drag ratio characteristics

Estimate the maximum lift coefficient:

The maximum lift coefficient depends on wing geometry, airfoil, flap geometry and its spread length, leading-edge slats and slats geometry, Re number, surface roughness, and influence from other components of the aircraft, such as fuselage, engine nacelles or pylon interference. The trim force provided by the flat tail will increase or decrease the maximum lift, depending on the direction of the trim force, and can also have an important effect on maximum lift under engine operating conditions if the propeller wash or jet wash hits the wings or flaps. Most aircraft use different flap states for takeoff and landing. During landing, the flaps are deflected to the maximum position to provide maximum lift and drag. However, the maximum flap deflection for takeoff can cause more drag than is expected during rapid acceleration and climb. As a result, the flaps will use about half the maximum deflection Angle, so that the maximum lift factor will be greater on landing than on take-off. In general, the maximum lift coefficient of take-off is about 80% of the maximum lift coefficient of landing. The table below lists typical C_{Lmax} values for some aircraft.[5]

Table 1.2.6: Typical value of maximum lift coefficient

Number	Aircraft type	C_{Lmax}	C_{LmaxTO}	C_{LmaxL}
1	Motor propeller aircraft	1.2-1.8	1.2-1.8	1.2-2.0
2	Single-engine propeller aircraft	1.3-1.9	1.3-1.9	1.6-2.3
3	Twin-engine propeller aircraft	1.2-1.8	1.4-2.0	1.6-2.5
4	Agricultural aircraft	1.3-1.9	1.3-1.9	1.3-1.9
5	Business aircraft	1.4-1.8	1.6-2.2	1.6-2.6
6	Turboprop regional aircraft	1.5-1.9	1.7-2.1	1.9-2.3
7	Jet conveyer	1.2-1.8	1.6-2.2	1.8-2.8
8	Military trainer	1.2-1.8	1.4-2.0	1.6-2.2
9	Fighter	1.2-1.8	1.4-2.0	1.6-2.6
10	Military patrol aircraft	1.2-1.8	1.6-2.2	1.8-3.0
11	Amphibious aircraft	1.2-1.8	1.6-2.2	1.8-3.4
12	Supersonic cruising aircraft	1.2-1.8	1.6-2.0	1.8-2.2

The aircraft designed in this paper is a supersonic cruise aircraft, so it is preliminarily selected $C_{Lmax} = 1.3,\ C_{LmaxTO} = 1.7,\ C_{LmaxL} = 1.9$.

1.3 Aircraft overall parameters detailed design

1.3.1 The choice of airfoil

The airfoil and its configuration on the wing have great influence on the aerodynamic characteristics. Therefore, it is possible to ensure the good aerodynamic characteristics of the wing only by selecting a good airfoil and correctly configuring it. In general, when designing an airfoil, the geometric data and aerodynamic parameters related to the airfoil should first be found out from the airfoil manual and other literature, and then comparative analysis is carried out to select the airfoil that can best meet the design requirements. [13]

There are many types of airfoils, which can be divided into high lift airfoils, laminar flow airfoils, supersonic airfoils, supercritical airfoils and low torque airfoils according to

their aerodynamic characteristics. Each type of airfoil has its advantages and disadvantages. The airfoil should be selected according to the requirements of the aircraft being designed.

Laminar flow airfoil is an airfoil designed to maintain a wide range of laminar flow on the boundary layer of the airfoil surface, thereby reducing drag. The characteristic of the airfoil is that the position of maximum thickness is backward. Aerodynamic characteristics: low resistance. More suitable for high subsonic aircraft.

High lift airfoils have higher lift coefficient and cruise drag comparable to other airfoils of comparable relative thickness. The common ones are NACA Group 44; NACA Group 24; NACA Group 230. Often used in low-speed general aviation aircraft. GAW-1- GAW-2 is an advanced airfoil for general aviation aircraft. For example, GAW-1 is characterized by a large upper surface leading edge to reduce the peak negative pressure at a large Angle of attack and delay airfoil stall. The upper surface is relatively flat, resulting in a uniform load distribution on the upper surface when the lift coefficient is 0.4. The lower surface has a large camber at the trailing edge.

Supercritical airfoil is a transonic airfoil suitable for supercritical Mach number aircraft. Its appearance characteristics are: the upper surface is relatively flat, the lower surface after the curve is larger, and upward concave, the head radius is larger. Aerodynamic characteristics: in the case of transonic flow, the shock wave intensity weakens obviously and is close to the trailing edge of the airfoil. The bow moment is large. Supersonic airfoil. In supersonic flight, in order to reduce wave resistance, the airfoil should have a sharp leading edge, so that the oblique shock wave generated can replace the positive shock wave in vitro. Aerodynamic characteristics: supersonic wave resistance is small, but because the sharp leading edge is easy to cause airflow separation, the subsonic performance is very poor. Generally symmetrical airfoil with relative thickness (t/c) of 3%-6%. Low torque airfoil: low head torque, even the direction of torque is upward direction. [14]

The aircraft designed in this paper is a supersonic cruise aircraft, for which the supersonic airfoil of NACA66 series, which is relatively mature at present, is selected. The shape of the airfoil is shown below:

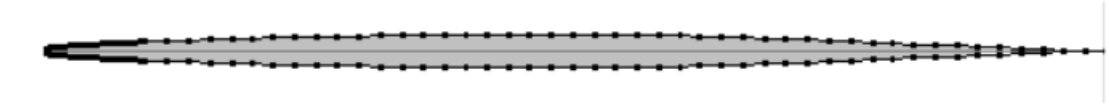

Figure 1.3.1 – NACA 66 – 003 airfoil

1.3.2 Fuselage design

The slender front fuselage of the aircraft can not only obtain higher low-speed elevation Angle lift, which is conducive to takeoff and landing, but also reduce the drag generated during supersonic flight, which is conducive to supersonic flight. The dimensions of the fuselage have several parameters: length, diameter, maximum cross-sectional area, and dimensionless slenderness ratio, including: fuselage slenderness ratio, nose slenderness ratio, tail slenderness ratio.

A typical scheme for increasing the slenderness ratio is to reduce the diameter for a given passenger aircraft seat or constant cargo floor area, while increasing the length of the fuselage. The aerodynamic drag of the fuselage varies in the other way.

For different fuselage arrangement schemes meeting these conditions, when diameter and length are variables, not only the seat number and cargo floor area are constant, but also the fuselage surface area is constant, S_f = constant. In this case, with the increase of slenderness ratio, the friction resistance can be considered constant, while the shape resistance will be reduced, so that the overall resistance D_f is reduced.

In the scheme of increasing the slenderness ratio, the drag coefficient will increase due to a sharp reduction in the cross-section area of the fuselage, making it beneficial to select the maximum fuselage slenderness ratio for aerodynamic characteristics in this scheme. When the slenderness ratio is increased, the wave drag generated during supersonic flight may be reduced, especially if the slenderness ratio is increased. The following figure shows the effect of fuselage slenderness ratio on drag.[15]

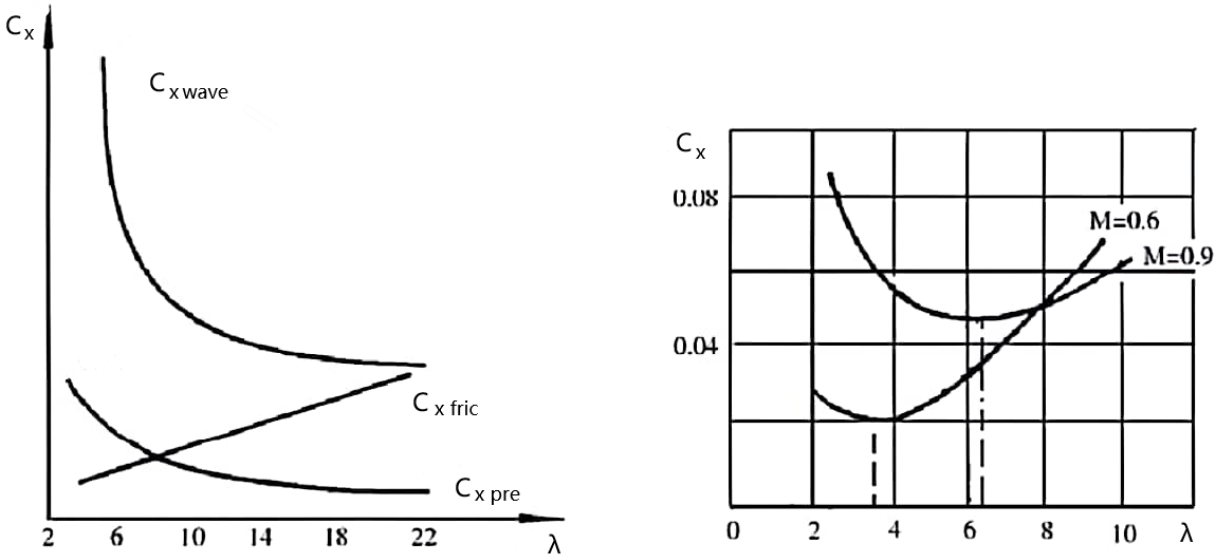

Figure 1.3.2.1 – Influence of fuselage aspect ratio on drag

As you can see from the picture：

(1) The pressure differential resistance and wave resistance of the fuselage decrease with the increase of λ.

(2) The friction resistance may increase with λ.

(3) The drag coefficient of the whole fuselage is related to M: When M=0.6, λ =3.5 is the most favorable; when M=0.9, λ = 6.5 is the most favorable, corresponding to a certain M, there is a certain most favorable slenderness ratio, and the higher M is, the larger λ is.

In the preliminary design process of aircraft, an initial value of fuselage slenderness ratio can be selected based on some empirical data and design indicators. The following is the statistical data of fuselage slenderness ratio selection. [16]

Table 1.3.1: Selection of fuselage aspect ratio (refer to statistics)

Aspect ratio	Low speed M<0.7	Hyper subsonic M< (0.8-0.9)	Supersonic
$\boldsymbol{\lambda_{fus}}$	6 - 9	8 - 13	10 - 20
$\boldsymbol{\lambda_{nose}}$	1.2 – 2.0	1.7 – 2.5	4 – 6
$\boldsymbol{\lambda_{tail}}$	2 - 3	3 - 4	5 - 7

According to the above theories and experiences, combined with the requirements of the supersonic business jet designed in this paper, the fuselage is preliminarily selected as a pencil-shaped fuselage with a aspect ratio of 10.8, a length of 40 meters and a maximum diameter of 3.7 meters.

Figure 1.3.2.2 – fuselage scheme

1.3.3 Wing design

In the whole aerodynamic design process of aircraft, the wing design is the most important. The wing is the main component for generating lift, but it can also house ammunition and fuel tanks, and retract landing gear during flight. According to the shape of the wing plane, the wing can be divided into: forward-swept wing (suitable for high-speed aircraft); Straight wing (suitable for low-speed aircraft); Swept wing (can be divided into single swept wing and double swept wing, suitable for high-speed aircraft); Delta wing (can be divided into single delta wing and double delta wing, suitable for high-speed aircraft); Diamond wing (for high-speed aircraft), curved leading edge wing (for high-speed aircraft), etc. In the design process of the wing, the first thing to meet the required design indicators, such as: the maximum lift required for take-off and landing state; The high lift-drag ratio required by cruising conditions, etc. [11] Therefore, the factors to be considered in aircraft wing design are:

1. The plane shape of the wing

When the flight Mach number of an aircraft reaches high subsonic velocity, compressibility effects appear, and the air flow accelerates through the upper surface of the wing, thus the local air flow reaches sonic velocity or even supersonic velocity. Shock waves are generated, and the shock waves induce boundary layer separation, resulting in a sharp increase in aircraft resistance. This is the phenomenon of drag divergence. It would make it difficult for the aircraft to increase its speed further. To solve this problem, forward-swept and back-swept wings can be used. They are therefore often used in supersonic aircraft.

2. The influence of plane parameters of wing on aerodynamic characteristics

(1). Aspect ratio λ

For low-speed aircraft, the induced drag decreases when the aspect ratio λ increases. For high-speed aircraft, wave resistance will increase when aspect ratio λ increases. As λ increases, the slope of the lift line increases. As λ increases, the stalling Angle of attack decreases. Reducing λ can prevent wing tip stall at large Angle of attack. Overall consideration, for supersonic aircraft: $\lambda = 3\sim5$, the minimum can be 2.

(2). Wing root-tip ratio η

According to Prandtl wing theory, when the lift distribution is elliptical, the induced drag is minimum. If the wing has no torsion and sweep, the lift distribution is elliptical and the induced drag is minimum when the plane shape of the wing is elliptical. When $\eta = 2.2$, the lift distribution is nearly elliptical, so many low-speed aircraft η is about 2.2. For supersonic aircraft, if the triangular wing is used, its wing root-tip ratio is large, then induced drag is no longer the main factor to be considered. For swept-back wing, the root-tip ratio of wing is considered mainly from the aspects of structural strength and stiffness. Therefore, $\eta = 3\sim5$ is generally selected for supersonic aircraft. [17]

(3). Sweep back angle χ

When χ increases, the critical Mach number can be increased and the generation of shock wave can be delayed. When χ increases, wave resistance decreases. As χ increases, the slope of lift line decreases. As χ increases, the maximum lift coefficient decreases. When χ increases, wing lift-drag ratio of K decreases. As χ increases, the weight of the wing structure increases. In general, for supersonic aircraft, when the subsonic leading edge is used, and when M=1.2~1.8, the corresponding $\chi = 40\sim60$, if χ is too large, the weight of the wing structure will be too large.

Leading international designs have selected a variety of wing layouts, including flat trapezoidal wings, variable sweep wings, large sweep delta wings or other delta wing variants. In this paper, it is believed that the trapezoidal flat wing produces the strongest sonic boom intensity, the trapezoidal swept-back wing produces much less sonic boom intensity, and the large swept-back delta wing produces the least sonic boom intensity. The wing design of the model supersonic business jet should be delta wing, which is

characterized by high stall critical point, faster flight speed, and can effectively reduce the problem of ultra-high-speed jitter.

The delta wing layout has a relatively large sweep Angle, which not only reduces the shock wave intensity of the leading edge of the wing, but also makes the shock wave position spread out along the axis of the aircraft to avoid the shock wave system gathered in the same station position. At the same time, the supersonic area law distribution of the aircraft with large swept delta wing layout is generally more uniform, avoiding the cross section with a sudden increase in cross section area, which is also beneficial to reduce the sonic boom intensity. For the aircraft with straight trapezoidal wing, the cross-sectional area of the wing position increases suddenly, which is not conducive to reducing drag and sonic boom. The effect of a trapezoidal swept wing is between a delta wing and a straight wing.

3. The influence of winglets

winglets can effectively improve aircraft fuel efficiency and increase cruising range.

When the air flows over the upper and lower surfaces of the wing, the difference in air pressure creates an upward lift on the wing. When this force is greater than the weight of the plane, the plane is able to fly through the sky. However, at this time, the high-pressure area air flow on the lower surface of the wing will bypass the wing tip and flow to the upper surface, forming a strong vortex air flow. The faster the aircraft flies, the stronger the vortex will be, which will increase the resistance and fuel consumption during flight.

The winglets realign the tip vortex further away from the outside of the wing and up above the laminar flow. After the wingtip winglets are installed, the wingtip vortices reconfigured by the wingtip winglets create a cross flow around the wingtip winglets, which is usually perpendicular to the flow over the wing surface. The lateral force generated by the cross-flow has a forward component that creates drag, and the winglets simultaneously generate thrust, effectively reducing drag and fuel consumption during flight.

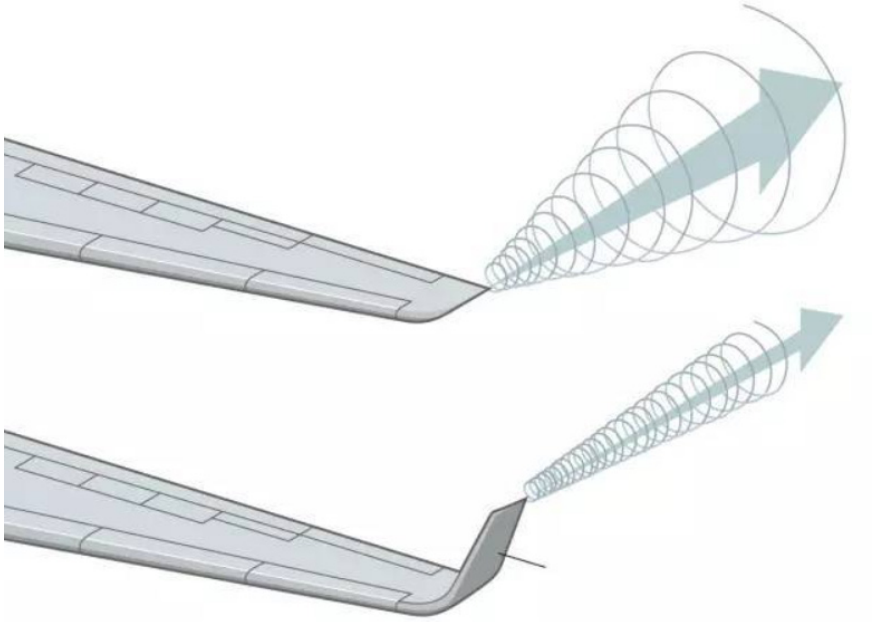

Figure 1.3.3.1 – The influence of winglets

According to the above theoretical basis, combined with the design indexes proposed in this paper, the aircraft wing in this paper is initially designed as a swept triangular wing with aspect ratio λ close to 4, wing root ratio η close to 3 and sweep Angle χ of 42 degrees. And it was added winglets. [18.19]

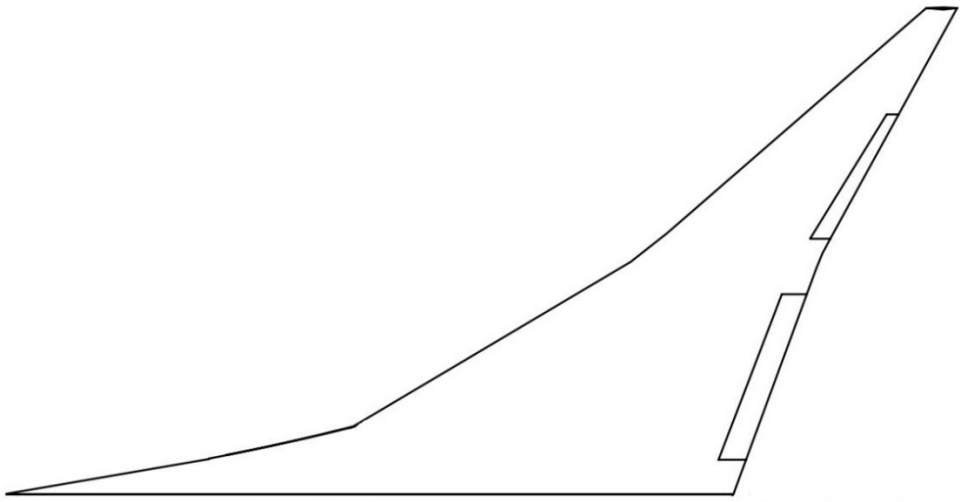

Figure 1.3.3.2 – back swept wing scheme

1.3.4 Aircraft control surface layout

The control surface of an aircraft is a movable surface hinged on an aircraft wing, horizontal stabilizer, and vertical stabilizer. They are used to control aircraft in flight and at high speed on the ground. Control surfaces include the main control surfaces such as elevators, full moving flat tail (slab tail), ailerons, rudder, auxiliary control surfaces such as leading slats, flaps, spoilers, and special control surfaces such as canards.

Ailerons are small pieces of movable airfoil mounted on the outside of the trailing edge of the wing tip. As the main steering surface of the aircraft, the roll moment generated by the pilot operating the differential deflection of the left and right ailerons can make the aircraft roll maneuver.

Rudder is the steerable wing part of the vertical tail, whose function is to yaw the aircraft.

Flaps increase lift during low-speed phases such as takeoff and landing, and allow for overall optimization of load, speed, drag, and fuel consumption.

We know that airplanes need enough lift to take to the sky. Increasing wing area or speed increases lift. However, in order to shorten the takeoff and landing distance and ensure the safety of the takeoff and landing process, the speed cannot be increased, and increasing the wing area will increase the weight of the aircraft. Flaps are a good way to solve this problem. Flaps increase lift in two ways:

(1). Increase the wing's relative camber and thick-aspect ratio.

(2). Increase the area of the wing.

Trailing edge flaps are movable wing surfaces that are mounted on the trailing edge of the wing, usually near the lower surface of the wing. In use, the flaps retreat along a slide mounted on the lower surface of the wing and deflect downward at the same time.

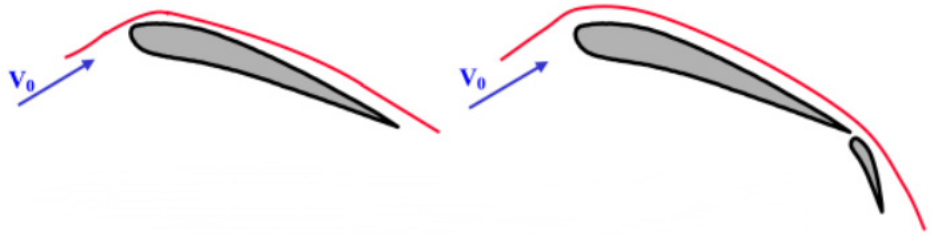

Figure 1.3.4.1 – Schematic diagram of the flap

Slab tail：In transonic and supersonic flight, the traditional flat tail trailing edge elevator greatly decreases its rudder efficiency under shock wave disturbance and cannot provide enough pitch control moment. Therefore, Slab tail is applied to greatly increase the elevator area in the way of overall deflection, so as to ensure the supersonic control efficiency.

Based on the above basic principles, the aircraft designed in this paper adopts the following control surface:

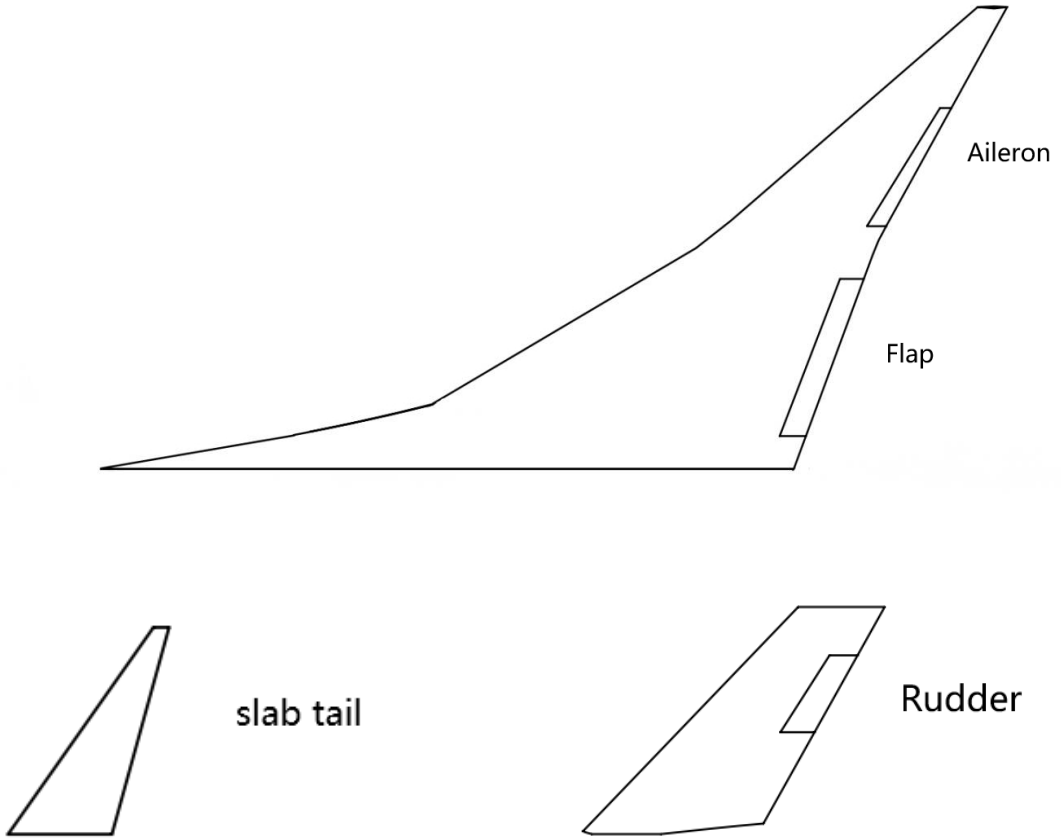

Figure 1.3.4.2 – control surface scheme

1.3.5 Design of power plant

(1). Engine position

The type of engine placement also has an effect on sonic boom strength. Different from fighter jets, business jets cannot accommodate engines inside the fuselage, so they can only be arranged outside the fuselage. Common engine layouts include Wing hoisting type, Tail hoisting type and inside wing root type.

If the engine is arranged in the wing root, it will cause loud noise in the cabin and heavy

structure. Modern aircraft rarely choose this layout form. Wing hoisting type and Tail hoisting type are not very different for sonic booms, depending on the shape of the wing.

Wing hoisting type has little influence on the fuselage structure, but requires the wing strength and stiffness to be better. For large swept delta wings, the Tail hoisting type can be selected.

It should be noted that no matter which layout is adopted, the installation position of the engine should be as far as possible to avoid the same section as the wing, otherwise the area law distribution will be affected. At the same time, in the section of the engine, attention should be paid to the fuselage modification, as far as possible to reduce the total cross-sectional area of this position.

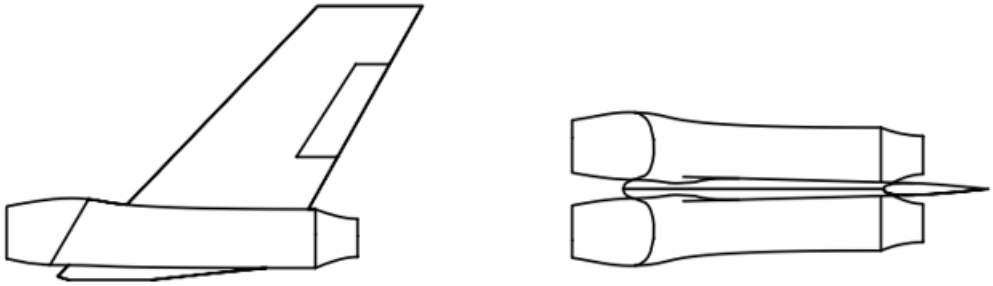

Figure 1.3.5 – Tail hoisting type power plant

(2). Choice of engine

There are four main categories of aeroengine: piston engine, gas turbine engine, ramjet engine and rocket engine. Gas turbine engine is the most widely used, which is generally composed of compressor, combustion chamber and gas turbine, including turboprop engine, turboshaft engine, turbojet engine and turbofan engine.

Piston engine：For aviation engines, the first is the piston engine, its working principle refers to the piston bearing gas pressure, repeated movement in the cylinder, and according to the connecting rod this movement into the rotating activities of the crankshaft. Piston aero-engines are generally not used in modern aircraft because of their inefficiency, but the rise of drones in recent years has brought them back into use.

Ramjet engine：Ramjet engine is a very simple structure, can send out a lot of thrust, suitable for high altitude and high-speed flight air jet engine. The method of compressed

air in this engine relies on the relative air flow of aircraft flying at high speed into the engine inlet to slow down and convert kinetic energy into pressure energy (for example, when the intake speed is 3 times the speed of sound, the air pressure can be theoretically increased by 37 times). During the operation of ramjet engine, high-speed air blows head-on to the engine, expands and slows down in the inlet, enters the combustion chamber and mixes with fuel oil (generally kerosene) after the pressure and temperature rise, and raises the temperature to 2000-2200℃ or even higher. The high-temperature gas then expands and accelerates through the propulsion nozzle, and is discharged at high speed from the nozzle to generate thrust. The thrust of a ramjet is related to the speed of the air intake. At three times the speed of sound, the static thrust generated on the ground can exceed 200 kN. It should be noted that ramjet has no compressor, cannot start in static conditions, so it is not suitable for ordinary aircraft power plant, and often used with other engines, become a combined power plant. It is mainly used as the power plant for intercontinental flying missiles.

Rocket engine：A rocket engine is a type of jet engine that turns propellant or reactive material into a high-speed jet that generates thrust due to Newton's Third Law. Rocket engines can be used for spacecraft propulsion as well as ground applications such as missiles. Most rocket engines are internal combustion engines, but there are also non-combustion engines. One of the hydrogen Scimitar engines is an environmentally friendly one that emits water vapor and nitrous oxide.[32]

Turbojet engine: The birth of the jet engine in Britain and Germany ushered in a new era of jet propulsion and aviation. The structure of a modern turbojet consists of an intake, a compressor, a combustion chamber, a turbine and a tail-nozzle, with an afterburner between the turbine and the tail-nozzle on a fighter jet.

The air first enters the engine inlet. When the aircraft is flying, the air flow can be regarded as flowing to the engine at the flight speed. Because the flight speed of the aircraft is changing, and the compressor adapts to the flow speed has a certain range, so the function of the inlet is to adjust the flow to the appropriate speed through the adjustable pipe.

The compressor after the inlet is specially used to improve the air pressure. When the air flows through the compressor, the working blade of the compressor does work on the air flow, so that the pressure and temperature of the air flow rise. At subsonic speeds, the

compressor is the main component of air pressurization.

The high-temperature and high-pressure gas flowing out of the combustion chamber flows through a turbine mounted on the same shaft as the compressor. Part of the internal energy of the gas expands into mechanical energy in the turbine, which drives the compressor to rotate. In a turbojet engine, the work done by the expansion of the air in the turbine is exactly equal to the work consumed by the compressor to compress the air and the work required by the transmission accessories to overcome the friction.

After combustion, the energy of gas in front of the turbine is greatly increased, so the expansion ratio in the turbine is far less than the compression ratio in the compressor. The pressure and temperature at the turbine outlet are much higher than that at the compressor inlet, and the thrust of the engine is derived from the energy of this part of gas.

The high-temperature and high-pressure gas flowing out of the turbine continues to expand in the tail nozzle and is discharged from the nozzle backward along the axial direction of the engine at a high speed. This speed is much greater than the flow of air into the engine, giving the engine a counteracting thrust.

Turbofan engine: Turbofan engine adds an external bypass and fan on the basis of turbojet engine, and the bypass ratio is not zero, so as to obtain more economical fuel efficiency. Turbofan engine is generally used in aviation passenger aircraft。

Turboprop/ turboshaft engine: Turboprop/turboshaft engine is a new type of power developed on the basis of piston engine after turbojet engine is born and mature. Turboprop engines replace piston propeller engines for fixed-wing aircraft and turboshaft engines replace piston shaft engines for rotor helicopters.

According to the proposed flight speed and other indexes of the designed aircraft, two hydrogen Scimitar engines are selected as power devices.

1.3.6 Design of landing gear

The landing gear is a takeoff and landing device that ensures the aircraft to skid, take off, land, skid after landing and maneuver through the airport. At this point, the landing gear sustains the loads acting on the aircraft and dissipates most of its kinetic energy during the landing skid.

Landing gear form refers to the number of fulcrum and its position characteristics relative to the center of gravity of the aircraft. At present, there are four types of landing gear used in aircraft: conventional landing gear, tricycle landing gear, bicycle landing gear with fulcrum under the wing and multi-point landing gear.

The landing gear in this paper is set to tricycle type, Rocker arm landing gear. Since the wings of the supersonic business aircraft designed in this paper are very thin, it is inconvenient to retract the landing gear into the wings, so the landing gear is placed on the fuselage reinforcing frame and the longitudinal rail.

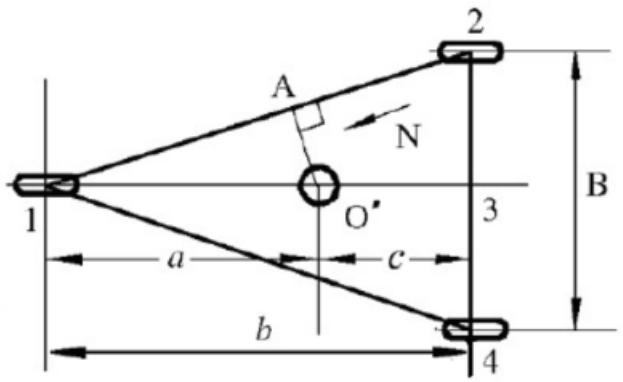

Figure 1.3.6.1 – Tricycle type landing gear

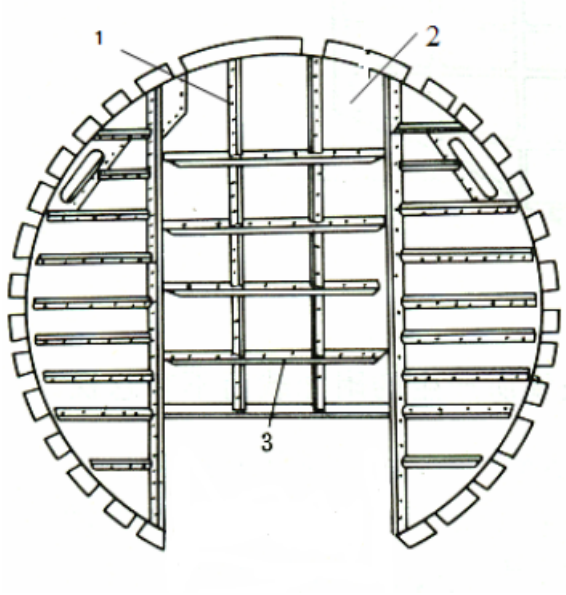

Figure 1.3.6.2 – Nose landing gear connection frame (Fuel tank frame)

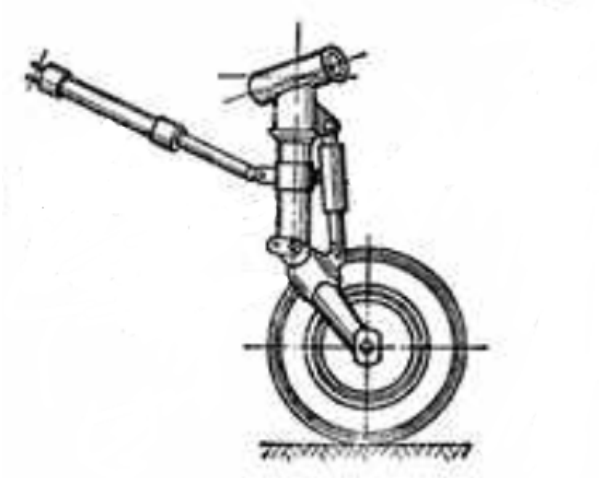

Figure 1.3.6.2 – Rocker arm landing gear

1.3.7 The design of the general configuration

(1). Windows should be designed to be as small as possible.

Subsonic aircraft generally fly at an altitude of 10,000 meters, sometimes also affected by clouds, air currents, often bumpy feeling. But flying above 17,000 meters, Concorde is largely unaffected by these weather factors, and at supersonic speeds, the plane is smooth. Concorde's cabin Windows are half the size of Boeing's, for two reasons: the first is insulation. By flying at twice the speed of sound, the fuselage produces friction with the air, making the surface temperature of the fuselage reach more than 90 degrees Celsius, and the ability of glass to protect against heat and radiation is less. Second, there is no view outside the cabin. Unlike subsonic aircraft, passengers can watch mountains and rivers rise and fall through portholes in clear weather. At supersonic speeds, there is only a faint blue light out of the porthole. So, the airplane windows should be as small as possible, or designed to be windowless.

(2.) The aerodynamic configuration of supersonic business aircraft designed in this paper is considered as follows:

In addition to the traditional T-tail placement, there are a number of layout methods

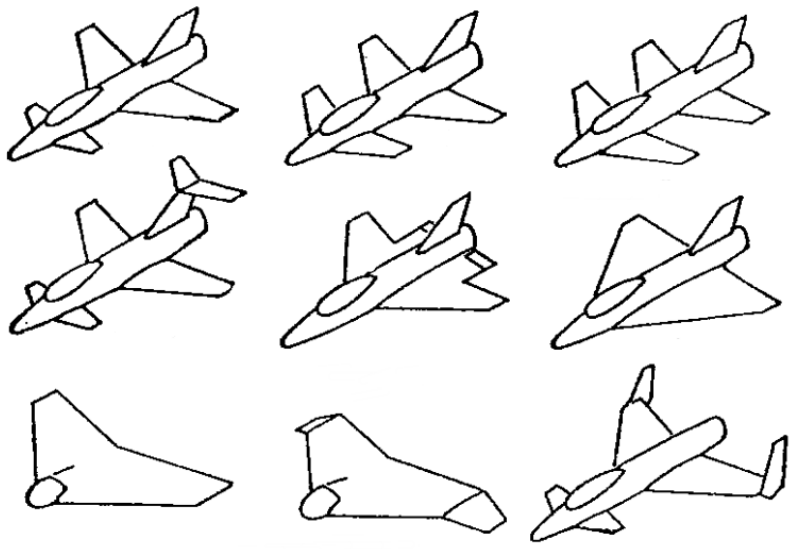

Figure 1.3.7.1 – Different tail layout methods

The international advanced scheme adopts both normal layout and canard layout. In this paper, the canard layout is better than the normal layout. In order to achieve aerodynamic balance, the normal layout of the flat tail brings negative lift and increases the load on the main wing, while the canard layout brings positive lift and reduces the load on the main wing. Since the sonic boom intensity contributed by lift is mainly related to the load on the main airfoil, so, the sonic boom intensity generated by the canard layout should be lower than that generated by the normal layout.

Table 1.3.7.1: Effect of configuration on sonic boom control

Component	Configuration	The ability to control sonic booms
Fuselage	Slender fuselage	excellent
	Stubby fuselage	bad
Main wing	Large Angle swept delta wing	excellent
	Trapezoidal swept wing	normal
	Trapezoidal flat wing	bad
Longitudinal control surface	canard layout	excellent
	Normal layout	normal

	Tail hoisting type	normal
Power plant	Wing hoisting type	normal
	Inside wing root type	uncommon

The effect of the layout of each location on the control of sonic boom is shown in the table above. It should be noted that the table mainly considered the need to control the strength of sonic booms, as well as some aerodynamic and structural strength design requirements. Model development also needs to balance the requirements of various aspects and choose the appropriate layout form.

It follows that the best layout for controlling sonic boom intensity alone is: slender fuselage + large sweepback delta wing + canard layout + Tail hoisting type engine.

(3). The consideration of the vertical position of the wing and the upper inverse Angle:

The vertical position of the wing relative to the fuselage is usually determined by the actual operating environment of the aircraft.

The main advantage of the high wing is that it allows the fuselage to be placed closer to the ground, which, in the case of military transport aircraft, allows cargo loading and unloading without specialized ground handling machinery. With the high wing, it does not need too long landing gear to ensure that the engine has enough clearance from the ground. There are two major disadvantages. The first is that the fuselage weight has to be strengthened in order to carry the landing gear load. The second is that for small aircraft, the high wing arrangement may block the pilot's view when turning or climbing.

The main advantage of the low wing design is that it is easy to place the landing gear inside the wing, since the wing casing is already strong enough that no additional load is required. Disadvantages: Having to add weight to the landing gear to ensure adequate clearance between the engine and the ground.

The center wing has the advantages of both the high wing and the low wing. The landing gear can be placed inside the wings without adding weight to the structure, and there is no possibility of block the pilot's view.

The upper inverse angle of the wing is the angle between the wing and the horizontal

line when viewed from the front. Whenever an aircraft tilts, the upper reverse angle tends to roll it over. This phenomenon occurs frequently and is often incorrectly interpreted as a result of the large projected airfoil area caused by subsidence. In fact, the rolling moment is caused by the sideslip generated by the angle of inclination. As the aircraft "slides" towards the sinking wing it increases its angle of attack. The resulting rolling moment is approximately proportional to the upper inverse angle.

The wing sweep angle also produces a roll moment associated with sideslip due to the change in the relative sweep angle of the left and right wings. For a swept wing, a negative moment is generated and is proportional to the sine of the sweep angle. This creates an effective inverse angle relative to the actual geometry.

Unfortunately, there is no simple method for selecting the upper inverse angle that takes into account all of these effects. Like many parameters in the initial design, the upper inverse angle can only be estimated from empirical data and then corrected in the analysis of the design layout below. Table 1.3.7.2 gives a preliminary estimate of the upper inverse angle.

Table 1.3.7.2: Upper inverse angle reference range

	high wing	Center wing	Low wing
No sweep (civil)	0 ~ 2	2 ~ 4	5 ~ 7
Subsonic swept wing	-5 ~ -2	-2 ~ 4	3 ~ 7
Supersonic swept wing	-5~0	-5 ~ 4	0 ~ 6

Based on the above principles, the supersonic business aircraft designed in this paper adopts the center wing, and the upper reverse angle is 3 degrees.

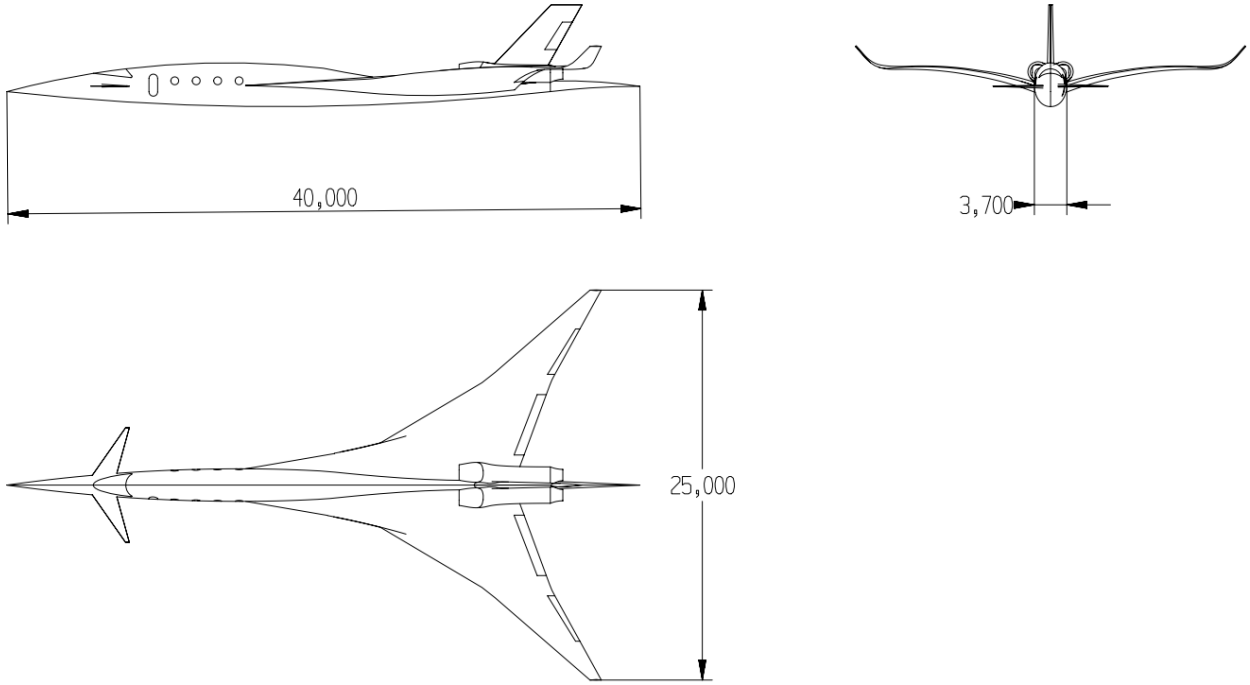

Figure 1.3.7.2 – Three views of designed aircraft.

2 Numerical Simulation of SSBJ 3D Model

2.1 Fundamentals of computational aerodynamics

Computational fluid dynamics (CFD) is widely used in the aerodynamic design of aircraft. It has a complementary relationship with wind tunnel tests. With the rapid development of computer, the status and role of CFD has been recognized accordingly. In the preliminary design stage of aircraft, CFD has become the main method of numerical simulation of aircraft, and wind tunnel experiment as the last check means.

In the detailed design stage of aircraft, it also provides an important calculation method for accurate calibration. The current aircraft design process ensures almost the same performance, but compared to wind tunnel experiments, the burden is much reduced, and the engineering cycle is shortened, saving design costs, thanks to the development and application of CFD. At present, the commonly used CFD software includes CFX, FLUENT. MGAERO, etc.

In the process of aircraft design, CFD is mainly used in the following areas:

(1) Aerodynamic design and aerodynamic analysis of aircraft under subsonic, transonic and supersonic conditions. The main data are as follows: surface pressure distribution of aircraft under different Mach numbers, different angles of attack and different attitudes, aircraft lift, drag, aircraft longitudinal torque, lateral torque and other important data.

(2) Design the airfoil according to the requirements of aerodynamic characteristics.

(3) Design the wing according to its optimal camber and twist distribution.

(4) Redistribute the load according to the aeroelastic requirements

(5) Calculation of unsteady computational fluid dynamics

(6) Calculation of internal flow such as inlet

(7) all-machine integrated pneumatic calculation

(8) Dynamic simulation of external weapon delivery process of aircraft

(9) Calculation of aerodynamic parameters of the leading edge and trailing edge flaps of the aircraft.

Although CFD numerical simulation has played a very important role in aircraft design, it cannot completely replace wind tunnel experiments, theoretical analysis and test flights. To be more accurate, these research means and methods need to cooperate and complement each other, so that they can jointly make more contributions to the improvement of aircraft design technology and the solution of related engineering problems. [8. 9]

2.2 Fundamental equations of the computational aerodynamics

2.2.1 Navaid Stokes (N-S) equations

The basic fluid governing equation consists of the laws of conservation of mass, momentum and energy, which are expressed as follows [20]:

$$\frac{\partial_\rho}{\partial_t} + \nabla \cdot \left(\rho \vec{V}\right) = 0 \tag{2.1}$$

$$\rho \frac{\partial_{\vec{V}}}{\partial_t} + \rho\left(\vec{V} \cdot \nabla\right)\vec{V} = \rho\vec{f} - \nabla \mathrm{p} + \nabla\left(\lambda \nabla \cdot \vec{V}\right) + \nabla \cdot \mu[\varepsilon] \tag{2.2}$$

$$\rho \frac{\partial_h}{\partial_t} + \rho\left(\vec{V} \cdot \nabla\right)\hbar = \frac{\partial_\rho}{\partial_t} + \left(\vec{V} \cdot \nabla\right)p + \Phi + \nabla \cdot (\mathrm{k}\nabla \mathrm{T}) \tag{2.3}$$

$$[\varepsilon] = \begin{pmatrix} 2\dfrac{\partial_u}{\partial_x} & \left(\dfrac{\partial_u}{\partial_y} + \dfrac{\partial_v}{\partial_x}\right) & \left(\dfrac{\partial_u}{\partial_z} + \dfrac{\partial_w}{\partial_x}\right) \\ \left(\dfrac{\partial_v}{\partial_x} + \dfrac{\partial_u}{\partial_y}\right) & 2\dfrac{\partial_v}{\partial_y} & \left(\dfrac{\partial_v}{\partial_z} + \dfrac{\partial_w}{\partial_y}\right) \\ \left(\dfrac{\partial_w}{\partial_x} + \dfrac{\partial_u}{\partial_z}\right) & \left(\dfrac{\partial_w}{\partial_y} + \dfrac{\partial_v}{\partial_z}\right) & 2\dfrac{\partial_w}{\partial_z} \end{pmatrix} \tag{2.4}$$

$$\begin{aligned} \Phi = \lambda(\frac{\partial_u}{\partial_x} + \frac{\partial_v}{\partial_y} + \frac{\partial_w}{\partial_z})^2 + \mu[2\left(\frac{\partial_u}{\partial_x}\right)^2 + 2\left(\frac{\partial_v}{\partial_y}\right)^2 2\left(\frac{\partial_w}{\partial_z}\right)^2 \\ + \left(\frac{\partial_v}{\partial_x} + \frac{\partial_u}{\partial_y}\right)^2 + \left(\frac{\partial_v}{\partial_z} + \frac{\partial_w}{\partial_y}\right)^2 + \left(\frac{\partial_u}{\partial_z} + \frac{\partial_w}{\partial_x}\right)^2] \end{aligned} \tag{2.5}$$

Where, Equation (2.1) is called mass equation or continuity equation, equation (2.2) is called momentum equation or N-S equation, and equation (2.3) is called energy equation.

From equation (2.1) to equation (2.3), there are six variables, $p, \rho, T, u, v, w,$ but from

equation (2.1) to equation (2.3), there are only five scalar equations. So, in order to be able to form the closed system, you have to add another equation. The gas equation of state can generally be used as a supplementary equation. The equation of state for a complete gas is expressed as follows:

$$p = \rho RT \tag{2.6}$$

If the fluid in question is air, the thorough force $\vec{f}$ of air is relatively small and can generally be ignored. μ and k represent the physical properties of the fluid, which can be known values in general, or as a function of temperature T. The N-S equations are the equations of motion governing the viscous fluid flow. [21] [22]

The motion of viscous fluid is divided into laminar flow and turbulent flow. Among them, turbulence is highly unsteady flow. Although in principle the N-S equation has been used to control the governing equations of turbulent flow, if the numerical calculation method is used to numerically simulate the real flow, then it needs to use a very dense grid to divide the diverging field, which will have high requirements on the computing speed and memory of the computer, and the current computer capacity cannot meet the requirements. In addition, it is not always necessary to describe the fluid so carefully in practical engineering. For some practical engineering problems, it is only necessary to know the value of a certain flow variable under the average time. For this reason, each variable of a turbulent flow is often regarded as the sum of its pulsation quantum and its average quantum. j changes rapidly with the passage of time, so people use the method of average value to study the turbulent flow condition. It is to take the time average value of each term in the N-S equation within the time interval far larger than the pulsation period of the flow, so as to obtain the differential equations of the mean value of the flow variable. The equations are called Reynolds equations. Also known as the Reynolds mean N-S system. [23]

After making certain assumptions about the time mean value of the product of each variable in the pulsation quantity (i.e., a certain "turbulence model"), the time mean value of each turbulent flow variable can be obtained by solving Reynolds equations. For incompressible turbulent flow, the corresponding Reynolds equations are expressed as follows:

$$\frac{\partial \vec{u}}{\partial_x} + \frac{\partial \vec{v}}{\partial_y} + \frac{\partial \vec{w}}{\partial_z} = 0 \tag{2.7}$$

$$\rho\left[\frac{\partial \vec{u}}{\partial_t} + \vec{u}\frac{\partial \vec{u}}{\partial_x} + \vec{v}\frac{\partial \vec{u}}{\partial_y} + \vec{w}\frac{\partial \vec{u}}{\partial_z}\right] = \rho f_x - \frac{\partial \vec{p}}{\partial_x} + \mu\nabla^2\vec{u} + \frac{\partial\left(-\rho\overrightarrow{u'u'}\right)}{\partial_y} + \frac{\partial\left(-\rho\overrightarrow{u'v'}\right)}{\partial_y} + \frac{\partial_{(-\rho\overrightarrow{u'v'})}}{\partial_z} \tag{2.8}$$

$$\rho\left[\frac{\partial \vec{v}}{\partial_t} + \vec{u}\frac{\partial \vec{v}}{\partial_x} + \vec{v}\frac{\partial \vec{v}}{\partial_y} + \vec{w}\frac{\partial \vec{v}}{\partial_z}\right] = \rho f_y - \frac{\partial \vec{p}}{\partial_y} + \mu\nabla^2\vec{v} + \frac{\partial\left(-\rho\overrightarrow{u'v'}\right)}{\partial_x} + + \frac{\partial_{(-\rho\overrightarrow{w'v'})}}{\partial_z} \tag{2.9}$$

$$\rho\left[\frac{\partial \vec{w}}{\partial_t} + \vec{u}\frac{\partial \vec{w}}{\partial_x} + \vec{v}\frac{\partial \vec{w}}{\partial_y} + \vec{w}\frac{\partial_{v\vec{w}}}{\partial_z}\right] = \rho f_y - \frac{\partial \vec{p}}{\partial_y} + \mu\nabla^2\vec{v} + \frac{\partial\left(-\rho\overrightarrow{u'v'}\right)}{\partial_x} + + \frac{\partial_{(-\rho\overrightarrow{w'v'})}}{\partial_z} \tag{2.10}$$

Where: $\nabla^2 = \frac{\partial^2}{\partial x^2} + \frac{\partial^2}{\partial y^2} + \frac{\partial^2}{\partial z^2}$

According to the comparison between the above equation and the incompressible N-S equation, the right side of the equation has 9 more terms related to the pulsation variable than the N-S equation. The mean value of these pulsating variables and the product of fluid density can be taken as a kind of stress in turbulent flow, which is called turbulent stress or Reynolds stress. In order to solve turbulent flow, it is necessary to add some expressions of mean value and turbulent stress in flow, which is called turbulence model. Turbulence model and turbulent flow are difficult problems in current fluid mechanics research and need further research. [24]

2.2.2 Euler's equations

For air and some fluids, their viscosity coefficient μ and heat conduction coefficient k are very small, which can be ignored, considered as $\mu = k = 0$. A fluid with this property is called an ideal fluid. In this way, equations (2.1) to (2.3) can be simplified into

EULER equations. If the flow is steady, the partial derivations of the flow parameters with respect to time are all 0. Euler's equations can be obtained by ignoring the complete force $\vec{f}$, as follows:

$$\nabla \cdot (\rho \vec{V}) = 0 \tag{2.11}$$

$$\rho \cdot (\vec{V} \cdot \nabla)\vec{V} = -\nabla \rho \tag{2.12}$$

$$\rho \cdot (\vec{V} \cdot \nabla)h = (\vec{V} \cdot \nabla)\rho \tag{2.13}$$

In some books, (2.12) is called Euler's equation, which is expanded along X, Y and Z to get:

$$\frac{\partial_u}{\partial_t} + u\frac{\partial_u}{\partial_x} + v\frac{\partial_u}{\partial_y} + w\frac{\partial_u}{\partial_z} = -\frac{1}{\rho}\frac{\partial_p}{\partial_x} \tag{2.14}$$

$$\frac{\partial_v}{\partial_t} + u\frac{\partial_v}{\partial_x} + v\frac{\partial_v}{\partial_y} + w\frac{\partial_v}{\partial_z} = -\frac{1}{\rho}\frac{\partial_p}{\partial_y} \tag{2.15}$$

$$\frac{\partial_w}{\partial_t} + u\frac{\partial_w}{\partial_x} + v\frac{\partial_w}{\partial_y} + w\frac{\partial_w}{\partial_z} = -\frac{1}{\rho}\frac{\partial_p}{\partial_z} \tag{2.16}$$

From equation (2.11) to equation (2.13), the total enthalpy of the fluid is H. Then, Bernoulli's equation can be obtained along the streamline:

$$\frac{\gamma}{\gamma - 1} \cdot \frac{p}{\rho} + \frac{|\vec{V}|^2}{2} = C\ (constant) \tag{2.17}$$

And we can also get Crock's theorem:

$$\nabla H = T\nabla S + \vec{V} \cdot \vec{\omega} \tag{2.18}$$

2.2.2 Boundary layer equation

In some areas of fluid flow, such as the thin layer of air near the surface of an aircraft wing, the viscosity and heat transfer of gases are important. This thin layer of air is called the boundary layer. In the boundary layer, the rate of change of fluid flow variable perpendicular to the boundary layer is much larger than that along the boundary layer, and

the velocity component perpendicular to the boundary layer is much smaller than that along the boundary layer. The study of boundary layer flow governing equation can be started from the N-S equation. According to the flow variable of boundary layer governing equation and the magnitude of its derivative order, some terms in the equations can be deleted, and then the boundary layer equation can be obtained. For example, if the flow is two-dimensional and the continuity equation is unchanged, the momentum equation and the energy equation can be written as:

$$\frac{\partial_u}{\partial_t} + u\frac{\partial_u}{\partial_x} + v\frac{\partial_u}{\partial_y} = \rho\left[-\frac{\partial_p}{\partial_x} + \frac{\partial}{\partial_y}\left(\mu\frac{\partial_u}{\partial_y}\right)\right] \tag{2.19}$$

$$\frac{\partial_p}{\partial_y} = 0 \tag{2.20}$$

$$\frac{\partial_h}{\partial_t} + u\frac{\partial_h}{\partial_x} + v\frac{\partial_h}{\partial_y} = \rho\left[\frac{\partial_p}{\partial_t} + u\frac{\partial_p}{\partial_x} + \frac{\partial}{\partial_y}\left(k\frac{\partial_T}{\partial_y}\right) + \mu\left(\frac{\partial_u}{\partial_y}\right)^2\right] \tag{2.21}$$

Where, equation (2.19) is the momentum equation in the x direction, equation (2.20) is the momentum equation in the y direction. Let's take x as the coordinates along the surface and y as the coordinates along the normal direction of the surface. According to equation (2.20), the pressure P in the normal direction along the boundary layer is a constant value, equal to p_1 at the outer boundary of the boundary layer. Since the viscosity is only considered inside the boundary layer and the viscosity outside the boundary layer is ignored, the relation between p_1 and velocity μ_1 and density ρ_1 at the outer boundary of the boundary layer can be obtained from the momentum equation (2.19):

$$\frac{\partial_{\mu_1}}{\partial_t} + \mu_1\frac{\partial_{\mu_1}}{\partial_x} = -\frac{1}{\rho}\frac{\partial_{p_1}}{\partial_x} \tag{2.22}$$

Due to the action of fluid viscosity, the velocity of the fluid relative to the object surface is zero at the object surface, which is called the condition of no slip on the object surface. At the same time, it needs to be explained that for an ideal fluid, the velocity component of the flow at the object surface is zero only in the normal direction of the object surface, and the tangential velocity along the object surface is still not zero, which is called the object surface no penetration condition.[25]

Although solving the boundary layer equation is much easier than solving the N-S equation directly, it is still very complicated. In practical engineering, people further developed the integral relation of the boundary layer, which can be integrated along the normal direction of the boundary layer through the equation of the boundary layer, and then by using some relations such as the continuity equation, the momentum integral form of the boundary layer can be obtained as follows:

$$\frac{d\delta^{**}}{dx}+\frac{\delta^{**}}{u_1}+\frac{d_{u_1}}{dx}(2+H+Ma_1^2)=\frac{c_f}{2} \tag{2.23}$$

Where:

$$H=\frac{\delta^*}{\delta^{**}} \tag{2.24}$$

$$c_f=\frac{2\tau_w}{\rho_1 u_1^2} \tag{2.25}$$

$$\delta^*=\int_0^\infty\left(1-\frac{\rho u}{\rho_1 u_1}\right)dy \tag{2.26}$$

$$\delta^{**}=\int_0^\infty\frac{\rho u}{\rho_1 u_1}\left(1-\frac{u}{u_1}\right)dy \tag{2.27}$$

$$\tau_w=\mu(\frac{\partial u}{\partial y})_{y=0} \tag{2.28}$$

After supplementing the relevant empirical formula and making some stipulations about the fluid velocity in the boundary layer along the normal direction, the integral formula of the boundary layer can be solved, and then every flow variable in the boundary layer can be obtained.

2.3 Common methods for calculating aerodynamics

(1) To solve the non-viscous linear fluid motion governing equations, these methods include: dipole grid method (belonging to the unsteady), the surface element method. Among them, the surface element method is used to solve linear equations. It divides many small surface elements on the surface and arranges them appropriately. It uses

boundary conditions to determine the strength of corresponding solutions, and then determines the aerodynamic characteristics and flow velocity of objects around the flow.

(2) Solving non-viscous nonlinear potential flow equations, such as solving full speed potential equation or transonic small disturbance potential flow equation using finite difference method. Like finite volume, finite difference method is also an important numerical simulation method in computational fluid dynamics (CFD), which is widely used. The principle of the finite difference method is that the derivative of the equations controlling fluid flow is replaced by the quotient approximation of the finite difference to obtain the difference equation. Under the conditions of the corresponding initial value and boundary value, the corresponding difference equation is solved by numerical calculation, and the numerical solution obtained is considered to be the original differential equation solution. [26]

(3) Solving non-viscous nonlinear euler equation + boundary layer equation correction, such as: finite element method, finite difference method, etc. Because the finite difference method is very strict to the shape of the grid, the finite element method which is not strict to the shape of the grid has been developed greatly. Because the finite element method does not require the shape of the grid harshly, it can satisfy the boundary conditions well. Its mathematical basis is the weighted margin method or the variational principle. For example, commercial aerodynamic analysis software MGAERO and FLUENT were developed using this method.

(4) To solve the N-S equation considering the effect of viscosity. When using this method, the turbulent stress term is mostly solved by semi-empirical formula, and then the finite volume method, finite difference method and other calculation methods are used to solve it. Wherein, the finite volume method means that the flow field to be calculated is divided into a finite number of small volumes, each of which is the control volume, and the control equations in the form of conservation integral are used. Therefore, the total divergence of each element can be replaced by the total product of vectors on the boundary surface of the element. [27] Using the difference method, the governing equations in the original integral form are spatially discretized into the time first order differential matrix equations of the average flow variables in the unit space. Then the time advance method is used to solve the problem.

(5) Grid generation. When using the above method to solve the governing equations, we need to solve the pre-processing problem first, which is called "grid generation technology". In the 1990s, a new grid generation technology called block structure grid method was developed, which can be directly interfaced with CAD, so it is easier to generate a relatively complex shape of computing grids. Later, it was found that the structural mesh could not meet the needs of the very complex shape mesh, so the Cartesian adaptive mesh and unstructured mesh were developed. An unstructured grid can get rid of the constraint of structured grid nodes, and its distribution of nodes and cells can be arbitrary, so it can handle boundaries well. In the process of grid generation, some optimization criteria are adopted to improve the quality of the grid generation. Meanwhile, the method can control the density of nodes and the size of the grid freely. Once you specify the distribution of the grid on the boundary, the grid is automatically generated between the two boundaries without chunking or intervention. Because of this, unstructured grid has been highly valued and developed in recent years. [28] [29]

2.4 Numerical methods for nonlinear aerodynamics

In the process of aircraft design, the overall design which is still in the early stage requires more accurate aerodynamic design and performance prediction. In order to meet this requirement, a new subject of computational fluid mechanics is established and developed on the basis of numerical computation, theoretical fluid mechanics and computer science.

Depending on the degree of simplification, The basic equations of compressible fluid dynamics can be divided into Euler equation, full potential equation, linear potential flow equation, nonlinear potential flow equation, N-S equation, etc. At present, the numerical simulation results of N-S equation are still very dependent on the assumption of boundary layer model. Therefore, the method of EULER equation plus boundary layer modification is still widely used in the aerodynamic design and aerodynamic characteristics analysis of aircraft in engineering practice. [30]

(1). Euler equation and its numerical solution

For example, let any variable in space that varies with time be R(x, y, t), where x and y represent space coordinates and t represent time coordinates, let $\Delta x, \Delta y, \Delta t$ respectively

corresponding coordinate system equidistant division, And the time is represented by the superscript n, t = nΔt, subscript i,j respectively corresponding when $x = i\Delta x, y = j\Delta y$, the value of R, so:

$$R_{i,j}^{n} = R(i\Delta x, j\Delta y, n\Delta t) \tag{2.29}$$

Where,Δx, Δy, Δt Respectively represents the grid size of the space grid and the corresponding time increment, using Taylor's formula to expand:

$$R_{i\pm1,j}^{n} = R_{i,j}^{n} \pm \left(\frac{\partial R}{\partial x}\right)_{i,j}^{n} \Delta x + \frac{1}{2}\left(\frac{\partial^2 R}{\partial x^2}\right)_{i,j}^{n} \Delta x^2 \pm \cdots \tag{2.30}$$

Finite differences can approximate derivatives, such as:

$$\left(\frac{\partial R}{\partial x}\right)_{i,j}^{n} = \begin{Bmatrix} \dfrac{R_{i+1,j}^{n} - R_{i,j}^{n}}{\Delta x} + o[\Delta x] & Forward\ difference \\ \dfrac{R_{i,j}^{n} - R_{i-1,j}^{n}}{\Delta x} + o[\Delta x] & Backward\ difference \\ \dfrac{R_{i+1,j}^{n} - R_{i-1,j}^{n}}{\Delta x} + o[\Delta x^2] & Central\ difference \end{Bmatrix} \tag{2.31}$$

Where, $o[\Delta x^m]$ Represents the magnitude of the truncation error of this expression is Δx^m。By analogy, the second partial derivative can be expressed as:

$$\left(\frac{\partial^2 R}{\partial x^2}\right)_{i,j}^{n} = \begin{Bmatrix} \dfrac{R_{i\pm2,j}^{n} - 2R_{i+1,j}^{n} + R_{i,j}^{n}}{\Delta x} + o[\Delta x] & Forward\ difference \\ \dfrac{R_{i,j}^{n} - 2R_{i-1,j}^{n} + R_{i-2,j}^{n}}{\Delta x} + o[\Delta x] & Backward\ difference \\ \dfrac{R_{i+1,j}^{n} - 2R_{i,j}^{n} + R_{i-1,j}^{n}}{\Delta x} + o[\Delta x^2] & Central\ difference \end{Bmatrix} \tag{2.32}$$

When using the above difference methods, it is necessary to determine the accuracy and stability of the calculation according to the physical meaning of the specific problem and the calculation results.[31]

(2). Boundary layer correction

With the assumption that the outside of the boundary layer is invisco-free, the governing equations of euler equation can be derived by using Newton's second law. A

similar method can be used to deduce the differential equations of viscous fluid in the boundary layer, but the viscous force must be added to the force of the fluid micro group, the boundary layer equation of the aircraft surface is established, and the equation is solved.

(3). Mesh generation method

In computational fluid dynamics, mesh generation technology is very important and indispensable content, and it is also the key technology that CFD can be effectively applied in practical engineering. In order to make the boundary conditions can be more accurately satisfied, the formation of body fitting mesh is one of the feasible methods, but for the aircraft with a more complex shape, it is very difficult to generate such a body fitting mesh, even if it is generated, it is relatively reluctant, and there is no way to guarantee the mesh quality. Therefore, partition computing and partition structure grid technology are often used at present, that is, the whole grid is divided into several small regions according to needs, and each small region is set up to solve the main control equation, and the solution of each small region is smooth on the boundary of its adjacent region through coupling conditions. The steps to generate a partitioned grid can be summarized as follows:

a. According to different shape characteristics and flow conditions, the regions are divided and the grid topology in each region is determined.

b. Generate the surface grid of the object - The surface grid of each component is distributed according to the requirements of mesh density in the geometric case.

c. Generating the interface meshes - the spatial location of the interface, its direction and the distribution of grid points on the interface will greatly affect the generation of the mesh and the quality of the final mesh.

d. Generation of spatial grids - After generating surface grids and interface grids, the boundaries of each region are determined. In principle, the spatial grids of each subregion can be generated by solving elliptic equations or algebraic methods.

With the needs of civil aviation transportation, the technical requirements of aircraft design are constantly improving, which requires more and more accurate aerodynamic calculation results and performance prediction. Therefore, CFD plays an increasingly important role in aircraft design. At present, numerical simulation has been able to replace flight test and wind tunnel test in some parts, and it has the advantages of short time, flexible

use and low cost. CFD numerical simulation is to give the numerical solution of the fluid flow range, rather than the exact solution. In addition, the mathematical formulas in practical engineering are usually complex multidimensional nonlinear partial differential equations, and the mathematical research required for numerical solutions is still insufficient, for example, some theories such as error, stability and convergence still lag behind the development of numerical simulation. Therefore, in numerical simulation, the reliability of numerical solutions needs to be verified together with wind tunnel test and physical theory analysis. [32]

2.5 Aerodynamic shape of model SSBJ

Supersonic cruise aircraft is a very complicated project, there have been several supersonic cruise aircraft in the aviation history, among which the more advanced Concorde has been retired because of various problems cannot be solved. In 2008, the European Space Agency was responsible for designing the aerodynamic layout of the new supersonic cruise transport aircraft, which was named the A2 Supersonic Cruise Passenger Aircraft.

It is designed to travel at five times the speed of sound. It can fly twice the speed of Concorde, can travel from Europe to Australia in less than 5 hours, can carry 300 passengers, in the ozone layer (about 30,500 meters above the sky) at Mach 5 (about 6,116 km/h), using the environmental hydrogen Scimitar engine, Length is 143 meters, width :45 meters, maximum range: about 20,117 kilometers. As A2 passenger aircraft is still in the preliminary stage of research, the available information is still limited. Therefore, this paper refers to the rough aerodynamic shape of A2 passenger aircraft, and on this basis, puts forward the overall index of the aircraft set in this paper and designs a supersonic business jet. The overall indicators proposed in this paper are as follows: The aircraft is equipped with two hydrogen Scimitar engines, range R=6,000 km, take-off weight $m_{0\,max}$=40 t, payload = 6 t, passenger number = 10 people, cruising altitude H= 3,000m, cruising Mach number Ma= 1.7.

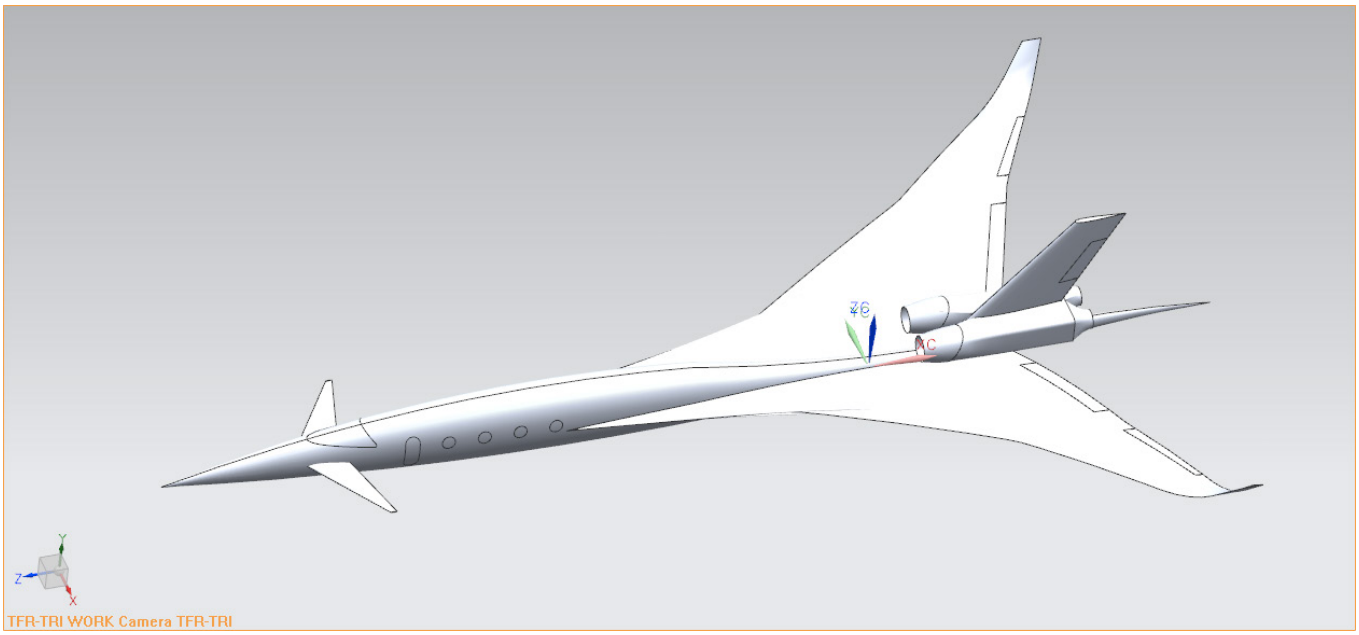

Figure 2.5.1 – Master geometry designed aircraft.

In this paper, three-dimensional software Siemens NX was used to complete the modeling of the aircraft model, which was output in STP format after completion and then imported into MESH for grid division. In this paper, the cruising altitude of the aircraft was set at 30,00m, the corresponding air density was 0.01841kg/m', and it belonged to supersonic flight.

The viscous resistance of the air accounted for a small proportion of the total resistance, so it could be assumed that there was no viscosity. Therefore, when dividing the body grids, boundary layer grids were not divided, and non-structural grids with strong adaptability were selected. In order to improve calculation accuracy, Size function is used to control grid generation during grid generation. The proportion of increase is 1.2. The grid is properly encrypted in places with drastic air flow changes, while the grid is sparse in other places with slow air flow changes.

This grid is of higher quality. In order to further improve the mesh quality and calculation accuracy, the adaptive mesh function of Fluent software is adopted in the calculation process, so that the software can automatically encrypt the mesh in the place where the pressure gradient changes greatly, while the place where the pressure gradient changes little automatically become sparse in the calculation process, so that the mesh can capture the shock wave more accurately. The calculated shock resistance is more accurate.

The following figure shows the calculation grid of the aircraft with initial profile in cruise state according to the above method. The calculation grid of other states is divided by the same method, and no redundant description is made here.

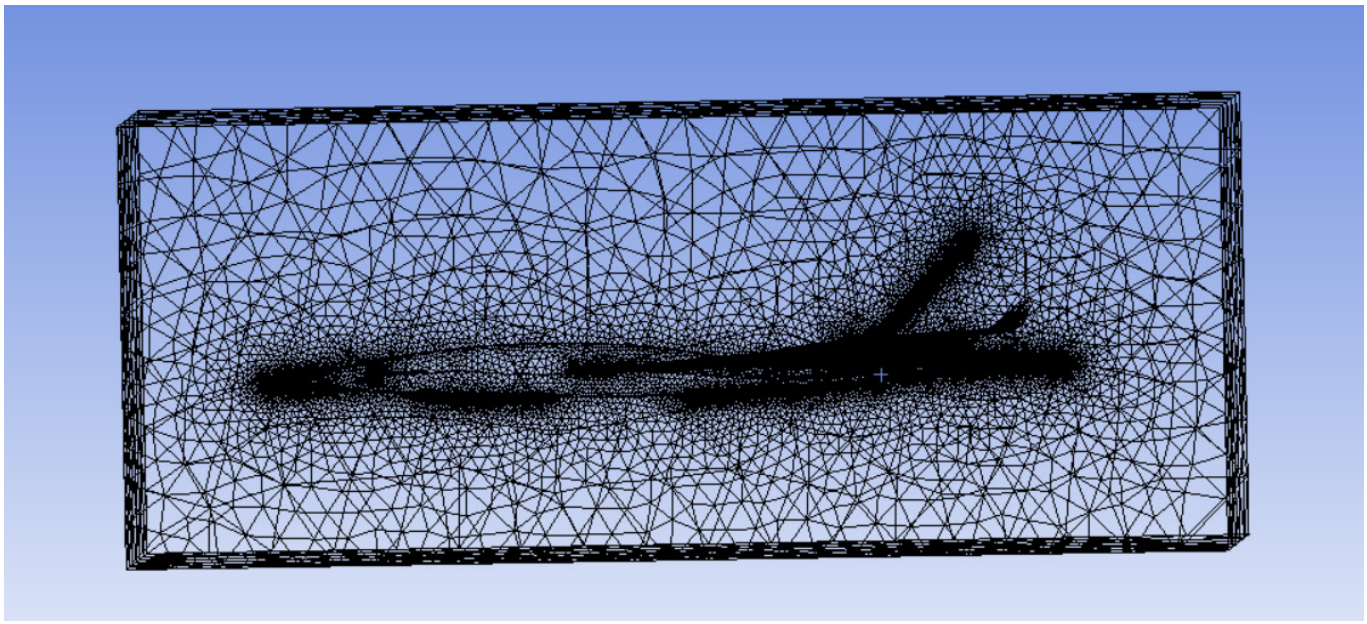

Figure 2.5.2 – General view of mesh.

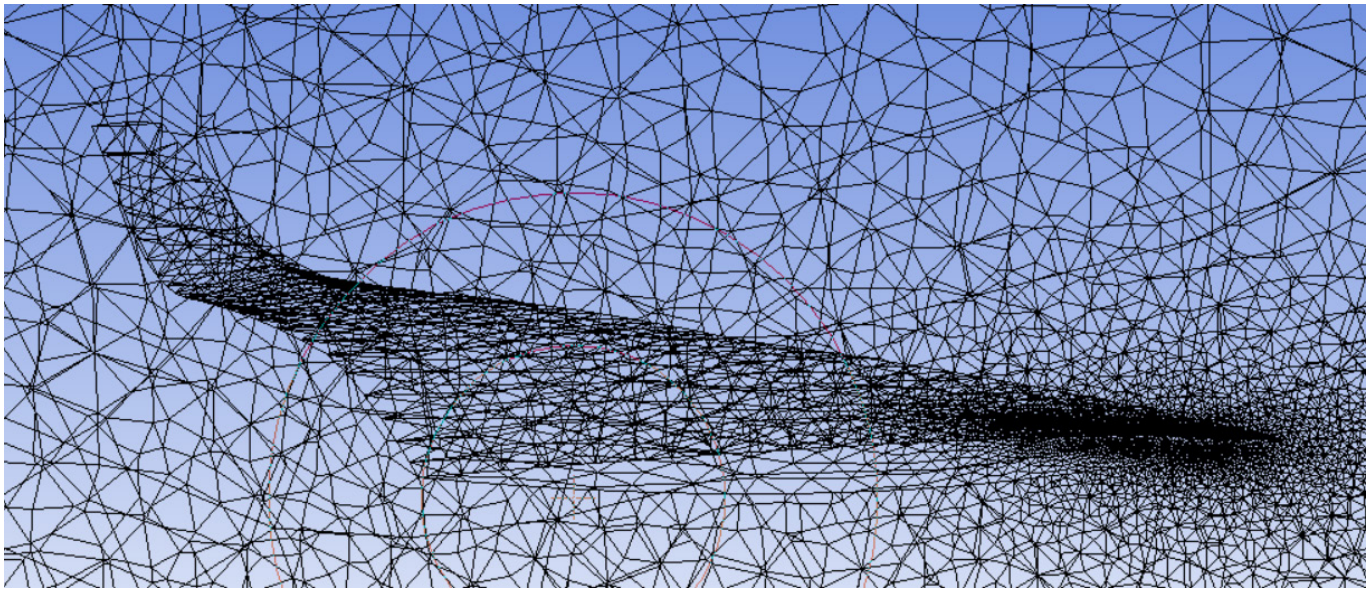

Figure 2.5.3 – Wing surface mesh.

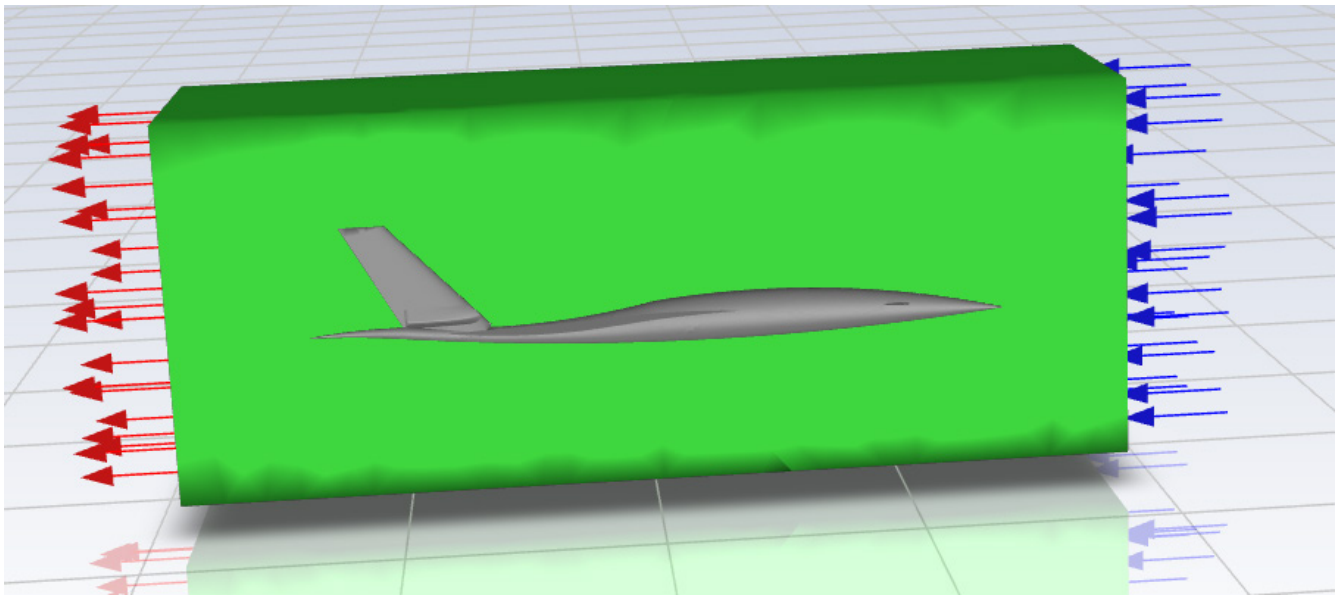

Figure 2.5.4 – Simulation diagram

3 Aerodynamic characteristics analysis of model SSBJ

3.1 Aerodynamic analysis during take-off and landing

(1). Data collation

During takeoff or landing, set the environmental parameters as: The height is sea level, the corresponding pressure is P=101325pa, and the temperature is T=300K, speed of sound is a=340m/s, density of air $\rho = 1.225\text{kg/m}^3$. As mentioned above, the weight of the supersonic aircraft designed in this paper is 40t at the beginning of take-off, and the weight ratio W_1/W_0 at take-off stage is 0.997, so the weight of the aircraft when taking off from the ground is 39.88t. The lift of the whole machine C is slightly greater than W_0, In the preliminary estimation, $\mathrm{C} \approx W_0$ can be taken, The lift force $C = C_L * 0.5 * \rho * V^2 * S$, After plugging in the data, the required lift coefficient of the whole machine is calculated $C_L \approx 0.2$, The center of gravity position is set 14m away from the head, and the average pneumatic chord length is 21.5 m, the reference area is the wing area $S = 65m^2$. In this state, the air density is relatively large, and the aircraft is flying at a low speed, so the viscous resistance of the air accounts for a large proportion of the whole aircraft resistance. In order to calculate the aerodynamic force of the whole aircraft more accurately, when FLUENT software is used in this state, the viscous force of the air is considered to solve the N-S equation, and the S-A turbulence model commonly used in aviation is selected as the turbulence model. By using FLUNET to calculate, it is found that when the aircraft Angle of attack is about 5 degrees, the required lift coefficient can be satisfied. At this time, the aircraft's velocity off the ground is about 367.2km/h, 0.3M, which is in line with the take-off speed requirements of general passenger aircraft. Here is the relevant aerodynamic analysis:

Table 3.1: Statistical table of aerodynamic parameters at T-O and Landing(0.3Ma)

Angle / Result	-3	1	5	8	12	16
C_L	-2.21E-01	5.71E-02	3.22E-01	5.10E-01	7.45E-01	9.61E-01
C_d	4.91E-02	4.11E-02	6.38E-02	9.84E-02	1.61E-01	3.07E-01
K	-4.50102	1.389294	5.047022	5.182927	4.627330	3.175896
Cm	7.50E-02	1.47E-02	-3.89E-02	-7.36E-02	-1.08E-01	-1.04E-01

According to the data in Table 3.1, draw: Angle of attack - lift coefficient diagram, Angle of attack - drag coefficient diagram, Angle of attack - lift-drag ratio diagram and Angle of attack - longitudinal torque coefficient diagram. They are as follows:

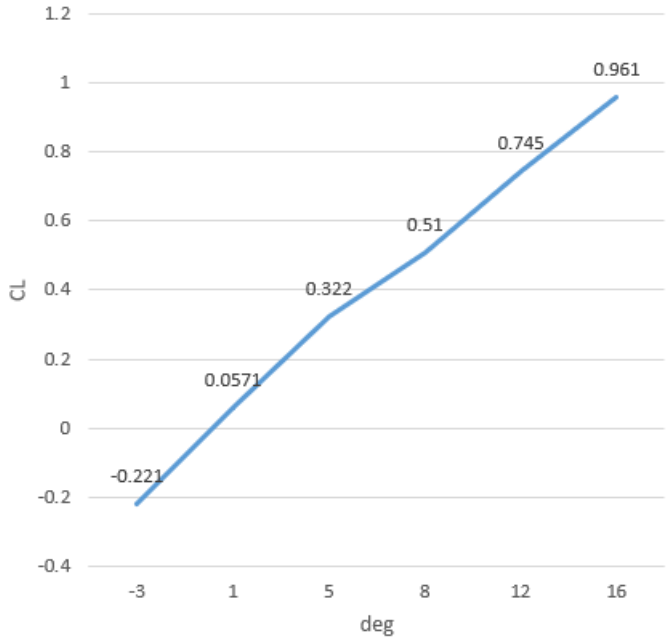

Figure 3.1.1 – Angle of attack - lift coefficient diagram

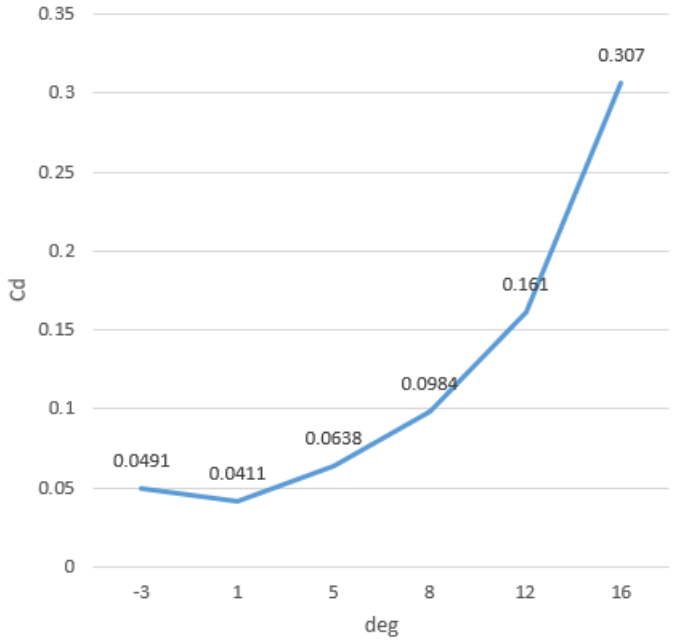

Figure 3.1.2 – Angle of attack - drag coefficient diagram

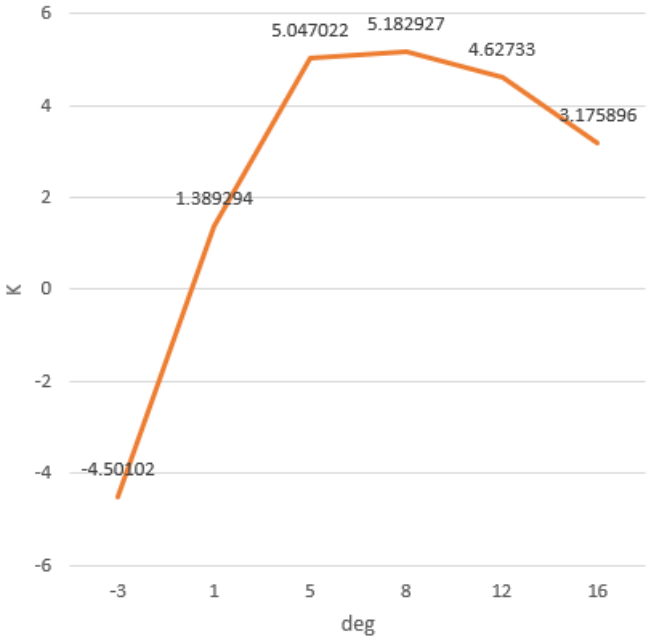

Figure 3.1.3 – Angle of attack - lift-drag ratio diagram

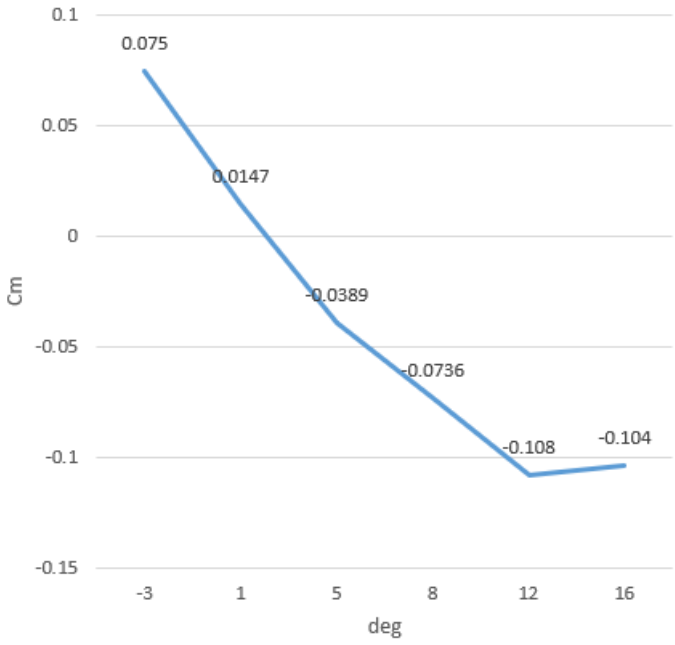

Figure 3.1.4 – Angle of attack - longitudinal moment coefficient diagram

(2). Result analysis

① It can be seen from Table 3.1 and Figure 3.1.1 that with the increase of the Angle of attack, the lift coefficient of the aircraft basically increases linearly, from negative lift at -3 degrees to 0.961 at 16 degrees. When the Angle of attack is 5 degrees, the lift coefficient

is 0.322, which has exceeded the lift coefficient required for take-off by 0.2. Therefore, from the perspective of lift coefficient, this design is successful. After the aircraft passes the cruise state, it enters the landing state. As mentioned above, the standby state weight ratio of the aircraft is 0.99, and the landing weight ratio is 0.995. After calculation, the weight of the aircraft after landing and completing the whole flight task is 32.5t. When the aircraft enters the landing state, the lift force C of the whole aircraft is slightly less than the gravity G, if C≈G is taken, if the velocity of the aircraft off the ground is still taken as the approach velocity of the aircraft in the landing state, Then by the formula $C = C_L * 0.5 * \rho * V^2 * S$, the lift coefficient required at this time is calculated $C_L \approx 0.16$, According to Table 3.1 and Figure 3.1.1, the aircraft's Angle of attack at this time is about 4 degrees, which can meet the requirements. As this paper is in the overall design, it does not take into account that the flaps will be opened to increase the lift of the aircraft during takeoff and landing. Therefore, when considering the situation after the flaps are opened in the detailed design, the required Angle of attack will be smaller.

② From Table 3.1 and Figure 3.1.2, it can be seen that in the range from negative Angle of attack to zero Angle of attack, the aircraft's drag coefficient decreases with the increase of the Angle of attack. In the range of positive Angle of attack, the aircraft's drag coefficient increases with the increase of the Angle of attack, and the slope of the drag coefficient increases with the increase of the Angle of attack. In the range of positive Angle of attack, from 0 degrees to 8 degrees, the resistance coefficient is obviously nonlinear with the change of the Angle of attack, and in the range of 8 degrees to 16 degrees, it is basically linear.

③ It can be seen from Table 3.1 and Figure 3.1.3 that, due to the inconsistency between the slope of lift coefficient and the drag coefficient when the lift coefficient changes with the Angle of attack, the lift-drag ratio k is not proportional to the change of the Angle of attack, but the maximum lift-drag ratio 5.18 is obtained when the Angle of attack is about 8 degrees.

④ As shown in Table 3.1 and Figure 3.1.4, since the center of gravity is in front of the aerodynamic pressure center and focus of the entire aircraft, the longitudinal torque coefficient of the aircraft decreases with the increase of the Angle of attack, and the bow moment is already present at a small Angle of attack. In addition, when the takeoff Angle

of attack and landing approach Angle of attack are about 5 degrees, the lower head moment is more reasonable, which is conducive to the flight safety of the aircraft. After this analysis, from this point of view, during takeoff and landing, the design of the aircraft is reasonable.

3.2 Aerodynamic analysis at high subsonic conditions

(1). Data collation

Under high subsonic conditions, environmental parameters are set as follows: at a height of 10000m, the corresponding pressure is P=26500pa, temperature is T=223.3K, sound velocity is a=299.5m/s, density ρ=0.4135kg/m^3. The center of gravity position is set 14m away from the nose, the average aerodynamic chord length is 21.5m, and the reference area is the wing area $S = 65m^2$.

The flying Mach number is 0.9M and the corresponding flying speed is 269.55m/s. In this state, the air density is small and the effect of air viscosity is weak, so the assumption of no viscosity can be made. When using FLUENT to calculate aircraft aerodynamic force, the three-dimensional EULER equation is solved without considering the air viscosity.

In order to obtain a high-quality mesh and capture the existence of shock waves without making the amount of mesh calculated too large, on the one hand, SIZEFUCTION method was used to control grid generation, the software generates a grid outward from the fuselage surface at a rate of 1.2; on the other hand, the mesh adaptive function is used in FLUENT.

Due to the appearance of shock waves, the pressure gradient of the place where shock waves are generated varies greatly, so the pressure gradient can be used as the judgment standard for mesh encryption and sparsity.

Since the yaw situation has not been considered in this paper, only half of the aircraft body grid is made when the aircraft body grid is made. The initial body grid is about 850,000. In the calculation process, the grid is about 890,000 after grid self-adaptation and automatic encryption. Here is the relevant aerodynamic analysis:

Table 3.2: Statistical table of aerodynamic parameters at 0.9M

Angle / Result	-3	1	5	8	12	16
C_L	-2.65E-01	7.06E-02	4.16E-01	7.04E-01	1.05E+00	1.30E+00

C_d	2.89E-02	1.68E-02	4.89E-02	1.06E-01	2.29E-01	3.82E-01
K	-9.16955	4.202381	8.507158	6.641510	4.585153	3.403141
Cm	1.09E-01	6.16E-03	-7.90E-02	-1.60E-01	-2.74E-01	-3.39E-01

According to the data in Table 3.2, draw: Angle of attack - lift coefficient diagram, Angle of attack - drag coefficient diagram, Angle of attack - lift-drag ratio diagram and Angle of attack - longitudinal torque coefficient diagram. They are as follows:

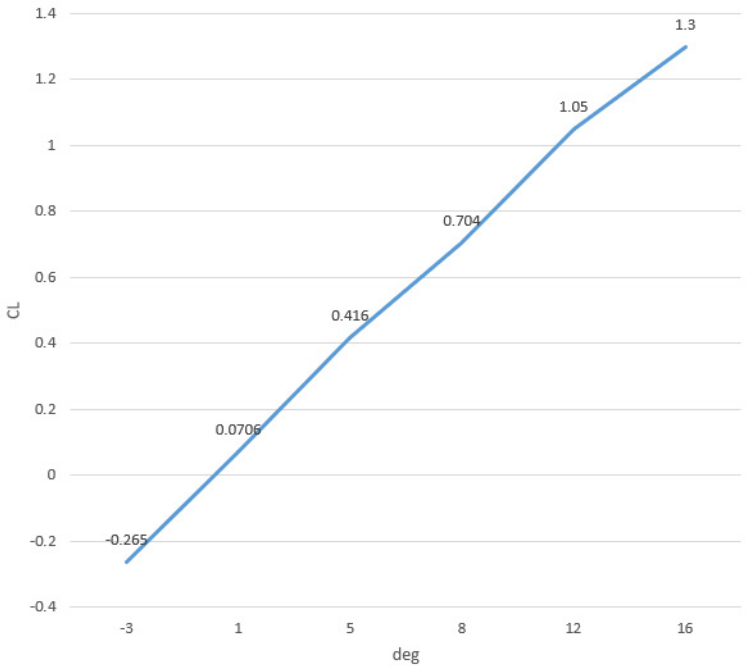

Figure 3.2.1 – Angle of attack - lift coefficient diagram

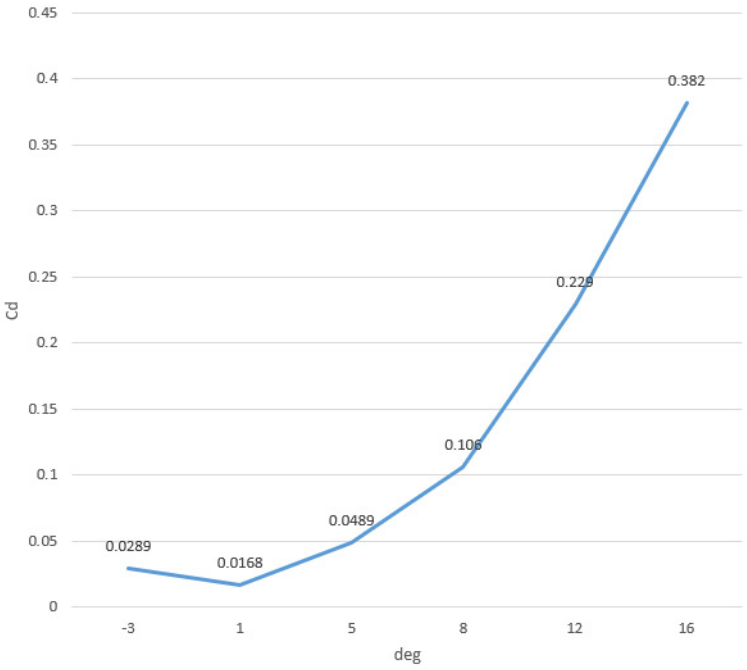

Figure 3.2.2 – Angle of attack - drag coefficient diagram

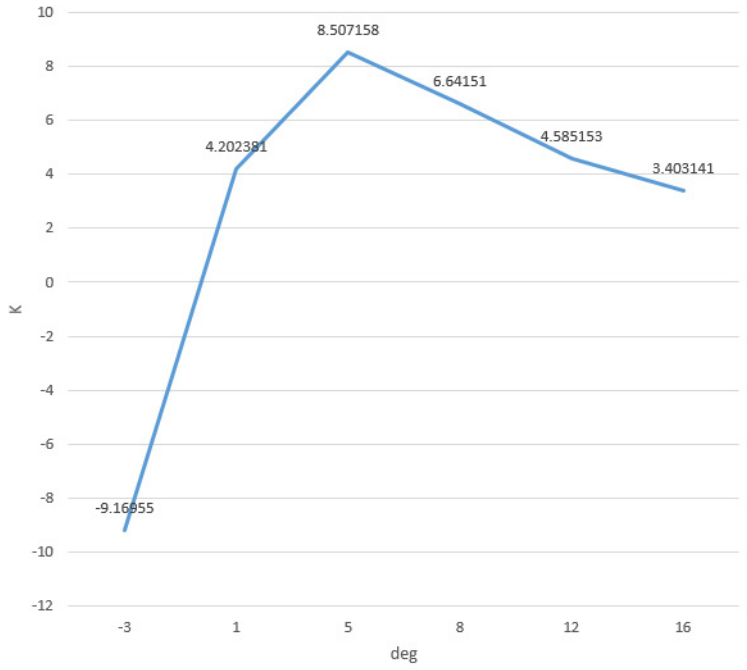

Figure 3.2.3 – Angle of attack - lift-drag ratio diagram

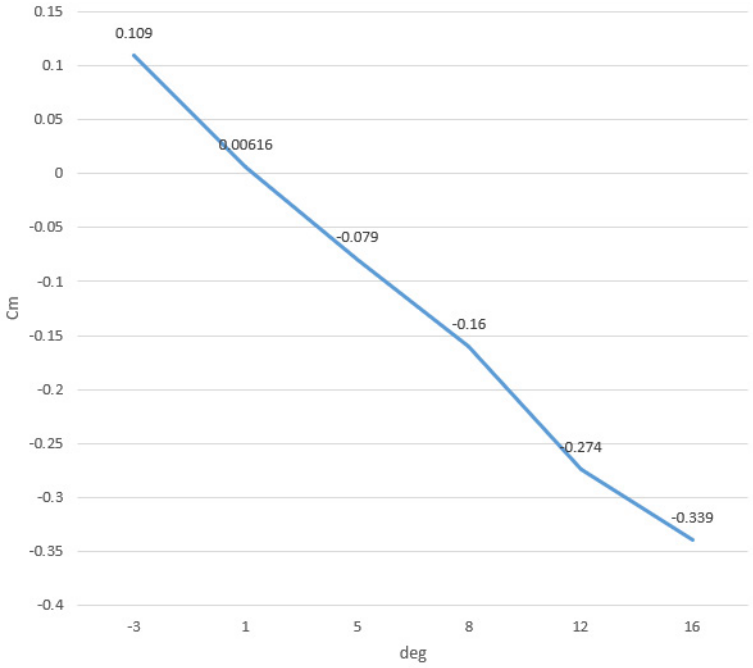

Figure 3.2.4 – Angle of attack - longitudinal torque coefficient diagram

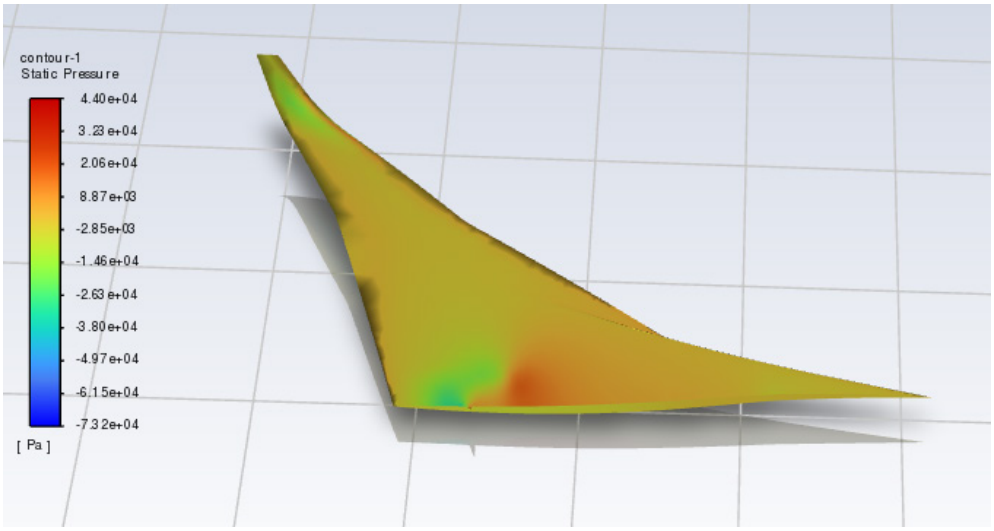

Figure 3.3 – Static pressure cloud image of wing surface (-3deg)

(2). Result analysis

① It can be seen from Table 3.2 and Figures 3.2.1-3.2.4 that the four parameters at 0.9M, such as lift coefficient, drag coefficient, lift-drag ratio and longitudinal torque coefficient, have the same variation trend with the increase of the Angle of attack as at 0.3M. Compared with the take-off and landing state, the longitudinal torque coefficient still decreases with the increase of the Angle of attack, and when it's less than 5 degrees of attack,

it's the bow moment. After the analysis, the aircraft design is reasonable at high subsonic speeds.

② According to FIG. 3.3, at an altitude of 10000 m, the aircraft flies at a speed of Ma=0.9, and local shock waves have been generated, and the intensity of shock waves increases with the increase of the Angle of attack. At the same time, it can be known from the static pressure cloud image that this calculation method is good for shock wave capture, which shows that it is very effective to capture shock waves by using mesh adaptive function when using FLUENT.

③ According to Table 3.1 and Table 3.2, at the same Angle of attack, when the Mach number is 0.9, the lift coefficient of the aircraft is about 30% higher than that at 0.3M. Since the aircraft has not reached the cruising altitude at this time, the large lift coefficient is very favorable for the aircraft to continue climbing to reach the cruising altitude.

3.3 Aerodynamic analysis in cruise condition

(1). Data collation

In the cruise state, environmental parameters are set as: the cruising altitude was set at 30000m, corresponding pressure P=1179pa, temperature T=226.5K, sound velocity a=301.7m/s, density ρ =0.01841kg/m^3. The cruising Mach number is 1.7M, the corresponding flight speed is 512.89m/s, Same as under 0.3M and 0.9M, in this state, 14m away from the nose is still taken as the center of gravity position, the average aerodynamic chord length is 21.5m, and the reference area is the wing area $S = 65m^2$. In this state, the air density is very small, and the effect of air viscosity is weak. As in the high subsonic state, the assumption of no viscosity can still be made. Mesh under 0.9M can still be used, just to more accurately capture the existence of shock waves. When mesh adaptive function is used in FLUENT, pressure gradient is still used as the judgment standard for mesh encryption and sparse, but the range of mesh encryption and sparse is appropriately changed. In this way, the grid is more strongly encrypted where shock waves are generated, which helps to capture shock waves. Practice has proved that this method can better capture the shock wave, and the amount of mesh is not too much. The imported mesh is about 850,000 initially, and about 980,000 after grid self-adaptation.

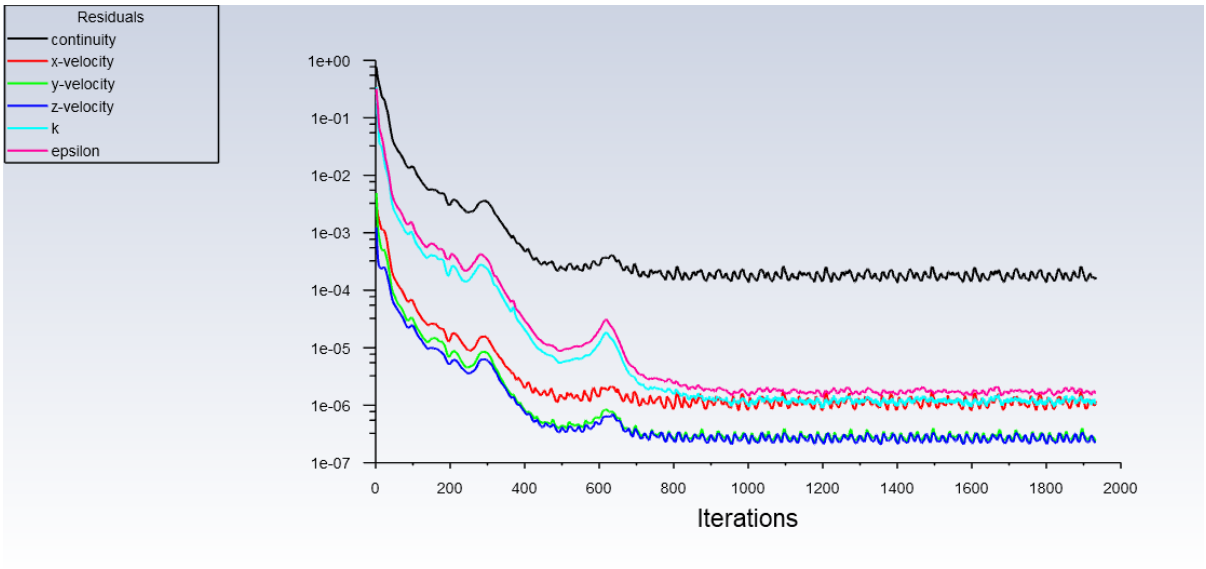

Figure 3.4 – Residual value convergence graph
(Before adding mesh adaptive)

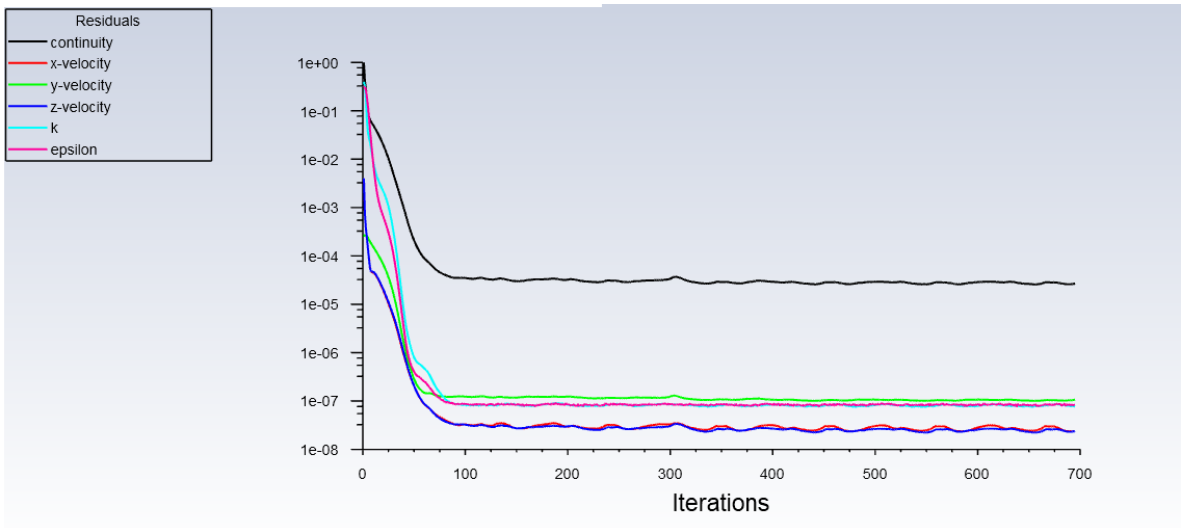

Figure 3.5 – Residual value convergence graph
(After adding mesh adaptive)

① It can be seen from Figure 3.4 that after about 100 steps, FLUENT readjust the grid according to the pressure changes of the calculated flow field to meet the needs of calculation. The convergence effect of the residual value is very good. After nearly 700 steps of calculation, the residual value has converged to the order of 10E-04, which proves that this method is very effective in calculating the flow field generated by shock waves.

② It can be seen from FIG. 3.5 that before mesh adaptive is added, the grid is not dense at the leading edge of the wing. Under supersonic flow, strong leading edge shock waves will be generated at the leading edge of the wing. The pressure gradient here is very

large, and mesh encryption is needed to better meet the shock wave capture. In this paper, after using FLUENT mesh adaptive function, the mesh at the leading edge of the wing is greatly encrypted.

Here is the relevant aerodynamic analysis:

Table 3.3: Statistical table of aerodynamic parameters at cruise condition

Result \ Angle	-3	1	5	8	12	16
C_L	-6.68E-02	4.04E-02	1.50E-01	2.37E-01	3.65E-01	5.13E-01
C_d	1.57E-02	1.30E-02	2.64E-02	6.90E-02	1.29E-01	1.69E-01
K	-4.255	3.108	5.682	4.333	3.388	3.036
Cm	2.91E-02	5.99E-03	-1.27E-02	-2.13E-02	-3.49E-02	-6.64E-02

According to the data in Table 3.3, draw: Angle of attack - lift coefficient diagram, Angle of attack - drag coefficient diagram, Angle of attack - lift-drag ratio diagram and Angle of attack - longitudinal torque coefficient diagram. They are as follows:

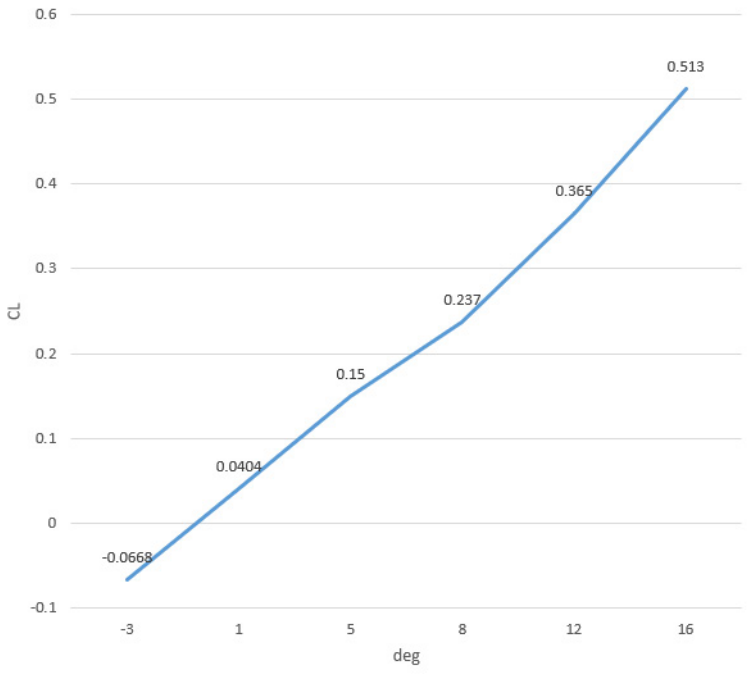

Figure 3.6.1 – Angle of attack - lift coefficient diagram

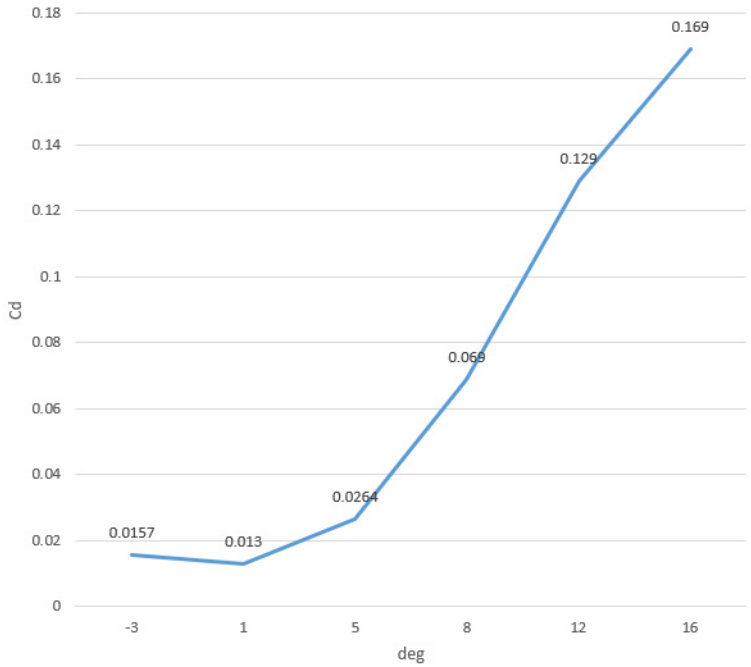

Figure 3.6.2 – Angle of attack - drag coefficient diagram

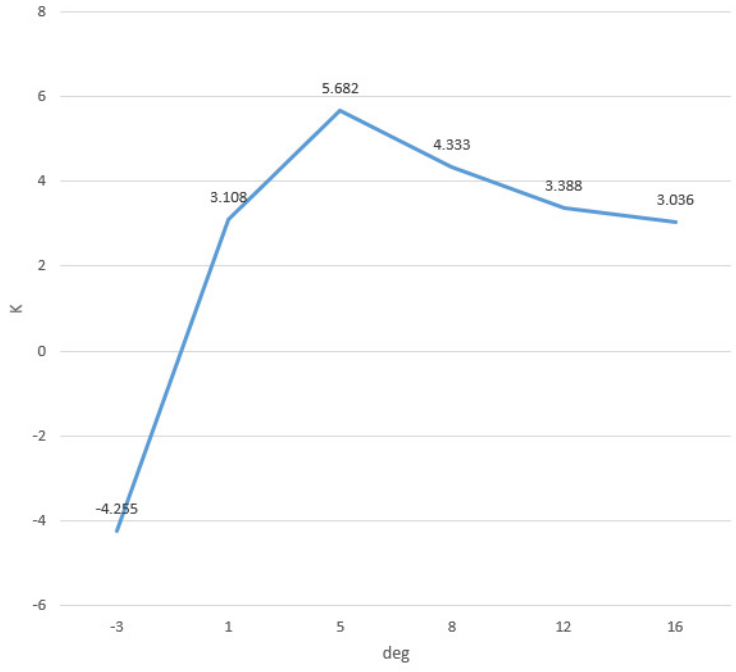

Figure 3.6.3 – Angle of attack - lift-drag ratio diagram

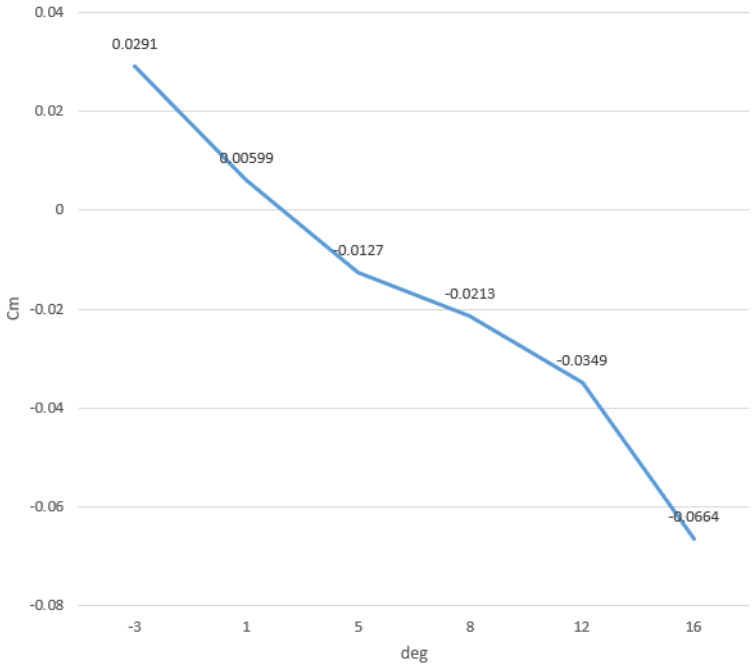

Figure 3.6.4 – Angle of attack - longitudinal torque coefficient diagram

(2) Result analysis

① As mentioned above, the weight of the supersonic business jet designed in this paper is 40t at the beginning of take-off, W_1/W_0 is 0.997 at take-off stage, W_2/W_1 is 0.985 at climb stage, the weight ratio of the cruise phase is 0.863, so it can be calculated that the weight of the aircraft at the beginning of the cruise is about 40t, and the weight at the end of the cruise is about 34.4t. In the cruise phase, the lift force C is equal to the weight W_0, C=W_0. By formula $C = C_L * 0.5 * \rho * V^2 * S$, The coefficient of lift required at the beginning of cruise is calculated by plugging in the data, C_L=0.317, Coefficient of lift required after cruise C_L=0.273, Therefore, the lift coefficient required in the cruise process ranges from 0.273 to 0.317. It can be seen from Table 3.3 and Figure 3.6.1 that the designed aircraft can meet the lift demand in cruise condition when the Angle of attack is between 9 and 11 degrees. After the end of cruise, the aircraft will be in standby state and then enter the landing state. As mentioned above, the weight ratio of the aircraft in standby state is 0.99. After calculation, the weight of the aircraft at the beginning of landing state is 33.3t, and the weight of the aircraft after landing and completing the entire aircraft task is 32.5t. When the plane enters the landing state, the lift force of the whole machine C is slightly less than the gravity G, if C≈G is taken, then by the formula $C = C_L * 0.5 * \rho * V^2 * S$,

the lift coefficient C_L ≈0.27 is calculated at this time. It can be seen from Table 3.3 and Figure 3.7.1 that the designed aircraft can meet the requirements when the Angle of attack is around 9 degrees.

② It can be seen from Table 3.2 and Table 3.3 that the variation trend of four parameters, namely lift coefficient, drag coefficient, lift-drag ratio and longitudinal torque coefficient, as the Angle of attack increases, is basically consistent with that under high subsonic flight condition.

③ It can be seen from Table 3.3 and Figure 3.6.4 that the designed aircraft profile is the bow moment within most of the Angle of attack, and at the cruising Angle of attack is the bow moment. In the whole flight process, the aircraft is in the cruise state for the longest time, the design of this stage is crucial to the success of the whole aircraft design. From this analysis, the design of this paper is successful.

3.4 Longitudinal stability analysis

When calculating the longitudinal torque of the aircraft profile, the center of gravity is taken as the reference point, and all the torques are relative to the center of gravity. The calculation formula is as follows:

$$\frac{m_z}{C_L} \times b_A = X_o - X_p \tag{3.1}$$

$$\frac{\partial_{m_z}}{\partial C_L} \times b_A = X_o - X_j \tag{3.2}$$

Where, X_o is the x-coordinate value of the reference point, let's say the center of mass is 14 meters, Longitudinal moment coefficient C_m used here m_z said, $X_p$refers to the X coordinate value of the center point of pneumatic pressure, $X_j$is the x-coordinate value of the focus of the aircraft. Analysis of the aerodynamic center and focus of the designed aircraft is as follows:

(1) In the take-off and landing state, the aircraft's flight Mach number Ma=0.3. At this time, at each Angle of attack, the m_z，C_L of the aircraft are shown in the following table:

Table 3.4: statistical table of pneumatic pressure center at 0.3M

Angle / Result	-3	1	5	8	12	16
C_L	-2.21E-01	5.71E-02	3.22E-01	5.10E-01	7.45 E-01	9.61 E-01
m_z	7.50E-02	1.47E-02	-3.89E-02	-7.36E-02	-1.08E-01	-1.40E-01
X_p(m)	16.041	12.452	14.726	14.868	14.871	14.876

According to Table 3.4, the trend diagram of longitudinal torque coefficient changing with lift coefficient is drawn, as shown below:

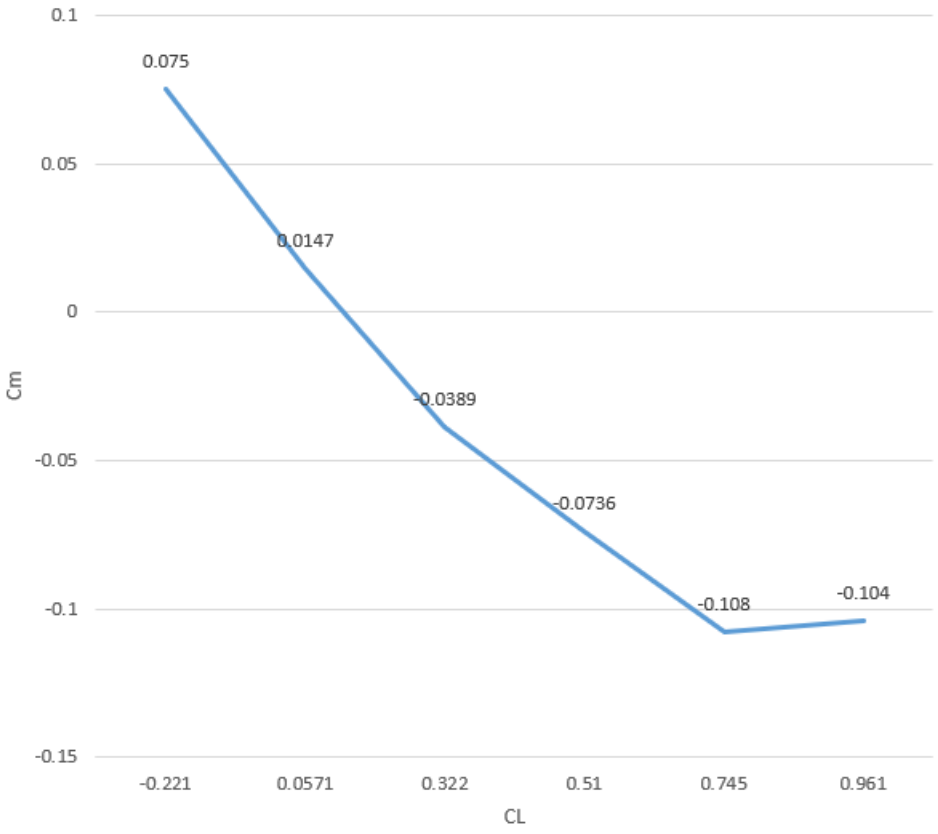

Figure 3.7 – Cm - CL diagram (Ma=0.3)

It can be calculated from Table 3.4 and Figure 3.7 that, $\partial_{m_z}/\partial C_L = -0.217$. Then, it can be obtained by substituting into formula (3.2), $X_j = 15.304m$, That is, the aerodynamic focus of the designed aircraft is about 15.304m away from the nose. In this case, the longitudinal static stability margin is $[(15.304 - 14)/14] * 100\% = 9.31\%$.

(2) At high subsonic conditions, aircraft flight Mach number Ma=0.9, At this time, at each Angle of attack, the m_z, C_L of the aircraft are shown in the following table:

Table 3.5: statistical table of pneumatic pressure center at 0.9M

Angle / Result	-3	1	5	8	12	16
C_L	-2.65E-01	7.06E-02	4.16E-01	7.04E-01	1.05 E+00	1.30 E+00
m_z	1.09E-01	6.16E-03	-7.90E-02	-1.60E-01	-2.74E-01	-3.39E-01
X_p(m)	16.474	13.475	15.142	15.367	15.289	15.288

According to Table 3.5, the trend chart of longitudinal torque coefficient changing with lift coefficient is drawn, as shown below:

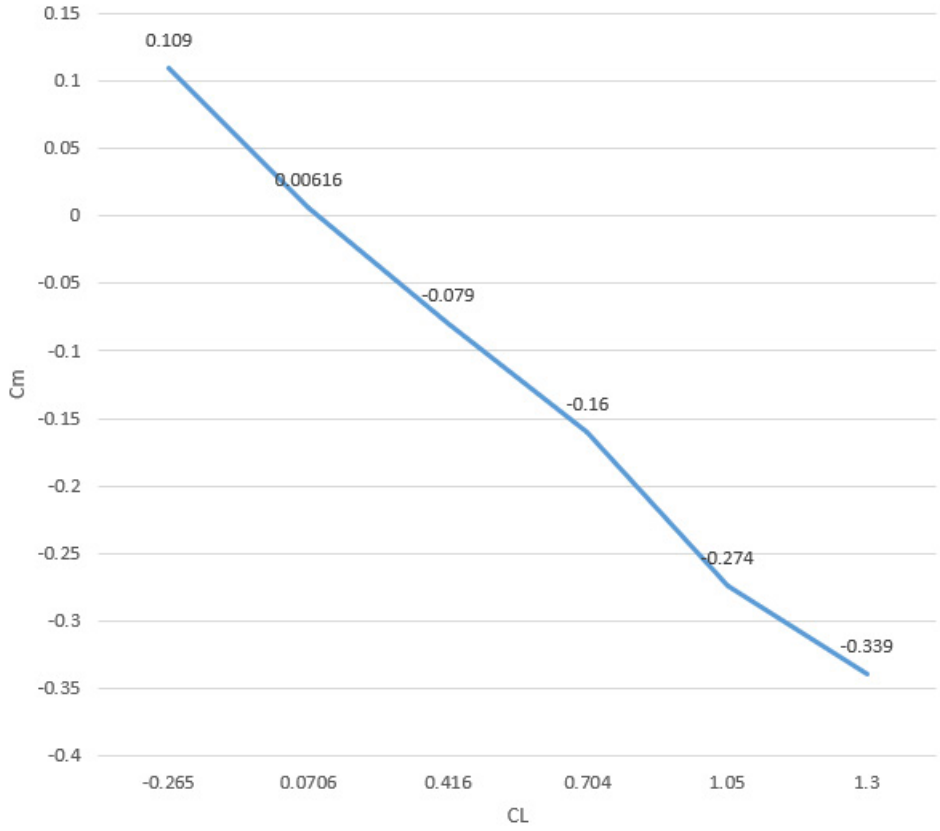

Figure 3.8 – Cm - CL diagram (Ma=0.9)

It can be calculated from Table 3.5 and Figure 3.8 that, $\partial_{m_z}/\partial C_L = -0.286$, Then, by substituting into formula (3.2), we can obtain: $X_j = 14.903m$, that is, the aerodynamic

focus of the designed aircraft is about 15.722m away from the nose. In this case, the longitudinal static stability margin is$[(15.722-14)/14]*100\%=12.3\%$.

(3) In the cruising state, the aircraft's flight Mach number Ma=1.7, At this time, at each Angle of attack, the m_z, C_L of the aircraft are shown in the following table:

Table 3.6: statistical table of pneumatic pressure center at 1.7M

Result \ Angle	-3	1	5	8	12	16
C_L	-6.68E-02	4.04E-02	1.50E-01	2.37E-01	3.65E-01	5.13E-01
m_z	2.91E-02	5.99E-03	-1.27E-02	-2.13E-02	-3.49E-02	-6.64E-02
X_p(m)	16.620	13.108	14.509	14.540	14.575	14.778

According to Table 3.6, the trend chart of longitudinal torque coefficient changing with lift coefficient is drawn, as shown below:

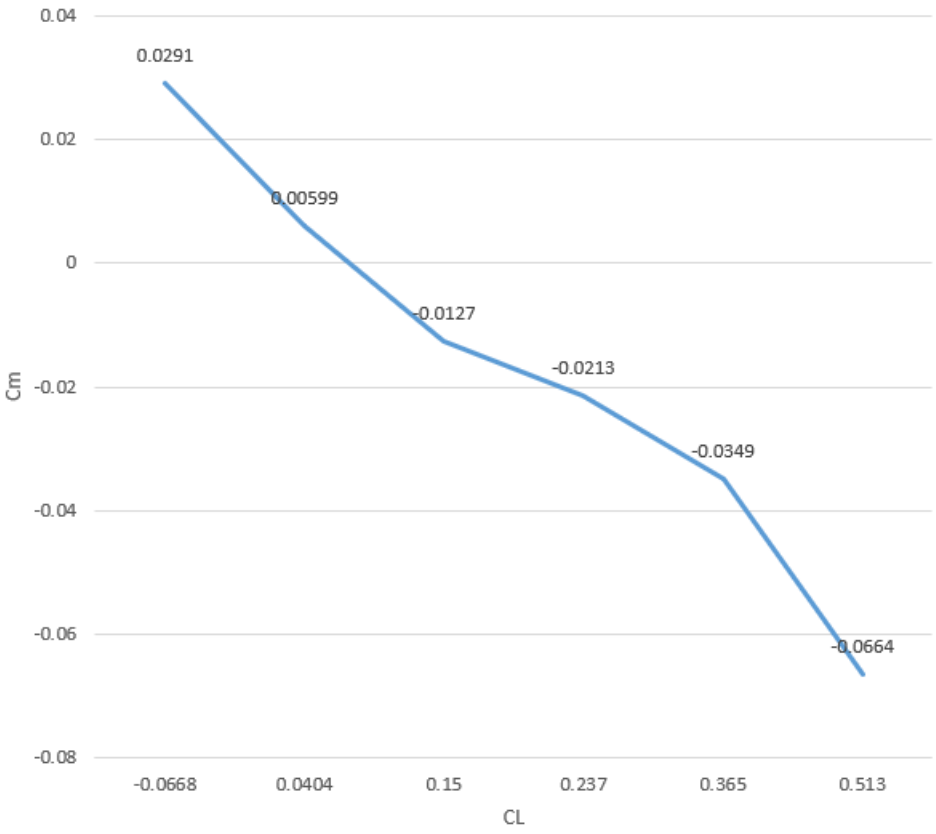

Figure 3.9 – Cm - CL diagram (Ma=1.7)

As can be calculated from Table 3.6 and Figure 3.9, $\partial_{m_z}/\partial C_L = -0.193$, Then, by substituting into formula (3.2), we can obtain: $X_j = 15.159m$, that is, the aerodynamic focus of the designed aircraft is about 15.159m away from the nose. In this case, the longitudinal static stability margin is $[(15.159 - 14)/14] * 100\% = 8.28\%$.

(4) Conclusion

The longitudinal stability analysis shows that the aircraft is statically stable during takeoff and landing, and the stability margin is 9.31%. At high subsonic velocity, the static stability margin is 12.3%. In the cruising state, the static stability margin is 8.28%. Through the above analysis, it can be concluded that the designed supersonic business jet meets the lift coefficient and lift-drag ratio required in takeoff, landing and cruise states, and the longitudinal stability of the aircraft in various flight states is largely satisfied, meeting the stability requirements of the aircraft. Therefore, the aircraft designed in this paper is feasible.

4 Economical Part

4.1 Calculation

The operating costs of this type of aircraft per 1:00 flight (flight hour) consist of direct and indirect (airport) expenses (formula (4.1)):

$$C_{op} = \mathrm{A} + B \tag{4.1}$$

Where A - direct costs per flight hour, dollars;

B - indirect costs per flight hour, dollars.

Direct costs include expenses for depreciation and overhaul and maintenance of an airplane (glider) and engines for fuel and flight personnel wages with accruals.

Indirect costs include depreciation, maintenance and maintenance of all aerodrome and airport facilities (bus stations, hotels, taxiways, parking lots, weather services, hangars, warehouses, roads, utilities, garages, etc.), excluding expenses for repair factories and linear workshops.

The total cost of operating the aircraft for the transport of passengers or commercial cargo per kilometer (CTKM) is determined by (formula (4.2)):

$$C_{TKM} = \frac{A + B}{m_{ld} \cdot k \cdot V_c} \tag{4.2}$$

Where $m_{ld} = 6000$kg, is the maximum payload of the aircraft;

V_c - airspeed;

K = 0.65 - utilization factor of the aircraft load.

The size of the speed of the aircraft is determined on the basis of its cruising speed. Flight (technical) speed is the average speed of a non-stop flight in calm, calculated taking into account the time spent at all stages of the flight from the start of acceleration at the landing airport. calculated speed by (formula (4.3)):

$$V_c = \frac{L \times V_{cr}}{L + (V_{cr} \times \Delta t)} \tag{4.3}$$

Where, V_{cr} =2000 km/h, cruising speed of the aircraft;

L = 6000 km - non-stop flight range;

t = 0.25 - loss of time for evolution or maneuvering in the airport area after take-off and before landing, as well as climb and decrease, which corresponds to a speed equal to cruising (in hours).

The magnitude of these losses depends on the altitude of the aircraft.

$$V_c = \frac{6000 \cdot 2000}{6000 + (2000 \times 0{,}25)} = 1846\ km/h$$

Direct expenses per one hour of flight, consist of the following expenses (formula (4.4)):

$$A = \sum_{i=1}^{7} A_i \tag{4.4}$$

Where A1 is the cost of depreciation and overhaul of the aircraft (glider)

A2 - expenses for depreciation and overhaul of engines;

A3 - maintenance and current repair costs for the airframe;

A4 - maintenance and current repair costs of power plants;

A5 - salary of flight personnel with accruals;

A6 - fuel cost;

A7 - other direct costs.

All Ai, we take per one flight hour.

The cost of depreciation and overhaul for one hour of aircraft operation, we define by (formula (4.5)):

$$A_1 = K_1 \times P_C \times \frac{1 + K_{RA} \times \left(\frac{T_C}{t_C} - 1\right)}{T_C} \tag{4.5}$$

Where K_1 = 1.065 - coefficient taking into account non-productive raid (instruction,

training, flight test, etc.).

P_c - price of an airplane without engines, dollars (formula (4.6)).

$$P_C = 0.015 \cdot K_{HBO} \cdot K_{CEP} \cdot K_V \cdot m_{ep} \cdot \left(3340 + 0.077 \cdot m_{ep} - 1{,}05 \cdot 10^{-5} \cdot m_{ep}^{1,5}\right) \quad (4.6)$$

Where K_{HBO}= 1.61

m_{ep} = m_{af}- (ml + m_{pp}) - mass of an empty plane.

m_{af} = 9600 kg - mass of the airframe;

ml = 280 kg — weight of the service load of the aircraft taking into account the weight of the crew;

m_{pp} = 4000 kg - mass of power plants;

m_{ps} = 9600 - (280 + 4000) = 5320 kg

coefficient taking into account the seriality of the designed aircraft (formula (4.7));

$$K_{CEP} = \left(\frac{35 \cdot 10^5}{m_{ep} \cdot \sum n_C}\right)^{0,4} \quad (4.7)$$

Where, $\sum n_C$=10, number of aircraft in a series;

$$K_{CEP} = \left(\frac{35 \cdot 10^5}{5320 \cdot 10}\right) = 65.79$$

coefficient taking into account the estimated flight speed of the designed aircraft (formula (4.8)).

$$K_V = \frac{1}{2} \cdot \left(1 + \frac{Vcr}{800}\right) \quad (4.8)$$

Where Vcr = 2000 km/h – aircraft cruising speed.

$$K_V = \frac{1}{2} \cdot \left(1 + \frac{2000}{800}\right) = 1.75$$

So, $P_C = 0.015 \cdot 1.61 \cdot 65.79 \cdot 1.75 \cdot 5320 \cdot (3340 + 0.077 \cdot 5320 - 1{,}05 \cdot 10^{-5} \cdot 5320^{1.5}) = 5540441.27$ Dollars.

KRA - coefficient showing the ratio of the cost of major repairs of the aircraft to the price of the aircraft (formula (4.9)).

$$K_{RA} = 0{,}11 + (3 \cdot 10^4 / P_c) \quad (4.9)$$

$$K_{RA} = 0{,}11 + (3 \cdot 10^4 / 5540441.27) = 0.115$$

for main aircraft on average:

TC = 30000 h;

tc =5000 h;

$$A_1 = 1.065 \cdot 5540441.27 \cdot \frac{1+0.115 \cdot \left(\frac{30000}{5000}-1\right)}{30000} = 309.78 \text{ dollars/hour}$$

Depreciation and overhaul expenses at one hour of engine operation, dollars / h, are determined by (formula (4.10)):

$$A_2 = K_2 \cdot n_{en} \cdot P_{en} \cdot \frac{1 + K_{REN} \cdot \left(\frac{T_{en}}{t_{en}} - 1\right)}{T_{en}} \quad (4.10)$$

Where K2 = 1,07 - coefficient taking into account non-production raid;

$n_{en} =$ 2 - the number of engines installed on the plane;

Pen - price of one engine, dollars (formula (4.11)):

$$P_{EN} = 61{,}183 \cdot K_{HBO} \cdot N_{Emax} \quad (4.11)$$

Where NEmax = 3800 kW - maximum engine power;

KHBO=1,61

PEN = 61,183 · 1,61 · 3800 = 374317,6 dollars.

$T_{en} = 6000$ h;

$t_{en} = 3000$ h;

K_{REN}=0.6;

$$A_2 = 1.07 \cdot 2 \cdot 374317.6 \cdot \frac{1+0.6 \cdot \left(\frac{6000}{3000}-1\right)}{6000} = 213.076 \text{ dollars. /h.}$$

The costs of current repairs and maintenance of the airframe (A3) and engines (A4),

dollars / h, consist of the costs of materials and spare parts, the wages of technical workers directly involved in the maintenance and repair of aircraft and engines, and are determined as follows (formula (4.12)):

$$A_3 = 0.024 \cdot K_3 \cdot K_4 \cdot \left(0{,}39 - 0{,}121 \cdot 10^{-5} \cdot m_{ep}\right) \cdot m_{ep} \qquad (4.12)$$

Where, K3= 0.61 - coefficient taking into account the maintenance method;

K4 = 2 - for aircraft with turbojet engine and turbofan engine;

mep = 5320 kg;

$A_3 = 0.024 \cdot 0.35 \cdot 2 \cdot (0.39 - 0.121 \cdot 10^{-5} \cdot 5320) \cdot 5320 = 34.28$ dollars/h

$$A_4 = \frac{0{,}024 \cdot 16 \cdot K_2 \cdot K_5 \cdot n_{en} \cdot \sqrt{R_{max}}}{1 + 7 \cdot 10^{-5} \cdot T_{en}} \qquad (4.13)$$

Where, K2= 1.07 - coefficient taking into account non-production plaque;

K5 = 1;

Rmax = NEmax = 3800 kW;

Ten = 6000 g.

$A_4 = \frac{0{,}024 \cdot 16 \cdot 1.07 \cdot 1 \cdot 2 \cdot \sqrt{3800}}{1 + 7 \cdot 10^{-5} \cdot 6000} =$ 35.67 dollars / h

The wage costs of flight personnel for one flight hour (A5), dollars / h, we consider, based on the number of passenger seats (formula (4.14)):

$$A_5 = 1{,}5 \cdot \left(0{,}9 \cdot n_{pass} - 0{,}00237 \cdot n_{pass}^2 - 2{,}9 \cdot 10^{-6} \cdot n_{pass}^3\right) \qquad (4.14)$$

Where, npass = 10 people - the maximum possible number of passenger seats on this aircraft;

$A_5 = 1.5 \cdot (0.9 \cdot 150 - 0{,}00237 \cdot 10^2 - 2.9 \cdot 10^{-6} \cdot 10^3) = 202$ dollars / h.

The fuel costs attributable to one hour flight (A6), dollars / h, we calculate by (formula (4.15)).

$$A_6 = 1{,}5 \cdot b \cdot P_k \cdot m_T \cdot n_{en} = \frac{\overline{m_T} \cdot m_0}{t_\Sigma \cdot n_{en}} \times P_k \qquad (4.15)$$

Where $\overline{m_T}$ = 0.26 - relative mass of fuel;

m0 = 40000 kg - take-off mass of the aircraft;

tΣ = 3 h - total flight time;

Pk = $ 1.5 / kg - the price of kerosene;

b = 1,045 - coefficient taking into account productive fuel consumption.

$A_6 = \frac{0.26 \cdot 40000}{3 \cdot 2} \times 1.5 = 2600$ dollars / h.

Other expenses for the aircraft (formula (4.16)):

$$A_7 = 0{,}07 \cdot \sum_{i=1}^{6} A_i \quad (4.16)$$

A_7 = 0.07·(309.78+213.076+34.28+35.67+202+2600) = 237.64 dollars / h.

Indirect costs (B) include depreciation, maintenance and maintenance of all aerodrome and airport facilities and the salaries of ground personnel (except the salaries of technical workers engaged in the maintenance and repair of the aircraft fleet).

Indirect costs depend on the class of the airfield and the number of take-offs and landings per hour of flight.

So, for this aircraft indirect costs will be (formula (4.17)).

$$B = 0{,}4 \cdot A_{\Sigma} \quad (4.17)$$

B = 0.4 · 3394.8 = 1357.9 dollars / h.

The operating costs of this aircraft per 1:00 flight (flight hour) are (formula (4.18)).

$$C_{OP} = A + B, \quad (4.18)$$

C_{OP} = 3394.8 + 1357.9 = 4752.7 dollars / h.

The total cost of operating the aircraft for the transport of passengers and commercial cargo per kilometer is calculated by (formula (4.19)):

$$C_{TKM} = \frac{A+B}{m_{ld} \cdot k \cdot V_c} \quad (4.19)$$

$$C_{\text{ТКМ}} = \frac{4752.7}{6 \times 0.61 \times 1846} = 70.34 \times 10^{-2}\ dollars\ /\ TKm$$

The revenue received by the aviation company from operating a fleet of aircraft of this type falls on one ton-kilometer, determined by (formula (4.20)):

$$\text{R}=\frac{P_{B\times n_{pass}\times K_3}}{m_{ld}\times V_c\times \tau} \tag{4.20}$$

$$\text{R}=\frac{830\times 10\times 0.61}{6\times 1846\times 6} = 76.18 \times 10^{-2}\ dollars\ /\ h$$

The profit earned by an aviation company from operating a fleet of aircraft of this type falls on one ton-kilometer, calculated by (formula (4.21)).

$$P_{rf} = R - C_{TKM} \tag{4.21}$$

$$P_{rf} = 76.18 \cdot 10^{-2} - 70.34 \cdot 10^{-2} = 5.84 \cdot 10^{-2}\ \text{dollars / TKm}$$

To determine the price of a ticket, provided that the operation of an aircraft of this class is break-even. We write the formula in the form (formula (4.22)).

$$R = \text{C}_{\text{ТКМ}} + P_{rf}, \tag{4.22}$$

WhereP_{rf}=0 (break-even condition),

and putting the unknown price of the ticket (CB) in revenue, we get:

$$P_B = \frac{m_{ld} \cdot V_c \cdot \tau \cdot \text{C}_{\text{ТКМ}}}{n_{pas} \cdot \text{К}_\text{З}}$$

$$= \frac{6\cdot 1846\cdot 6\cdot 70.34\cdot 10^{-2}}{10\cdot 0.61} = 7663\ dollars$$

$$\frac{P_B \times 10 \times 0.61}{6 \times 1846 \times 6} = 0.7034$$

P_B= 7663 dollars

With a margin of 25%, ticket price:

P_B= 1.25×7663 = 9579 dollars

4.2 Conclusion

In this section, we calculated the costs of operating the aircraft and the engine at

$ 35.67 / h and the cost of transporting one ton of cargo per kilometer, and determined the price of the ticket, which amounted to $ 9579. The indirect costs for one hour of flight are $ 1357.9 / h.

5 Future Prospects

4.1 Blended wing body will be considered in the future

Designed as a wing-body hybrid, the SSBJ is a concept that could revolutionize aviation technology. The advantages of wing-body fusion are light weight, large internal volume and small aerodynamic resistance, which can greatly improve the flight performance of aircraft. At present, there are many technical obstacles to overcome. With the deepening of research work, more and deeper key technologies are bound to be put forward. At the same time, it is believed that more and more attention is paid to the research of wing-body fusion supersonic aircraft. Through a large number of theoretical and experimental research, these key technologies can be breakthrough.[8][13][17]

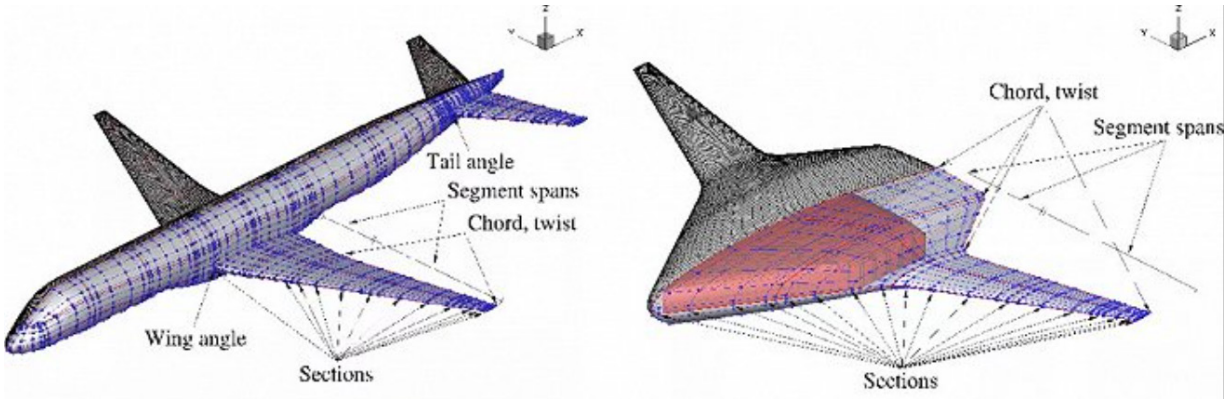

Figure 4.1 – Blended wing body

4.2 Use scramjet engines as the power plant

Scramjet is a ramjet in which fuel is burned in supersonic airflow. When using hydrocarbon fuel, scramjet flight Ma number is below 8, when using liquid hydrogen fuel, its flight Ma number can reach 6~25. Supersonic or hypersonic air is diffused in the inlet to a lower supersonic speed of Mach 4. Fuel is then injected from a wall or a projection in the air stream, mixed with air and burned in the supersonic combustion chamber, and finally the burned gas is discharged through an expanded nozzle. The advantages are reduced environmental pollution and high combustion efficiency. The disadvantage is that the ramjet cannot be started in a stationary condition. So, the future is going to be a combination of ramjets and turbojets. A hybrid engine under study, for example, would place a turbojet inside a ramjet's intake. Turbojets are used for take-off; ramjets start at M=0.4 and are

designed to fly at four times the speed of sound.

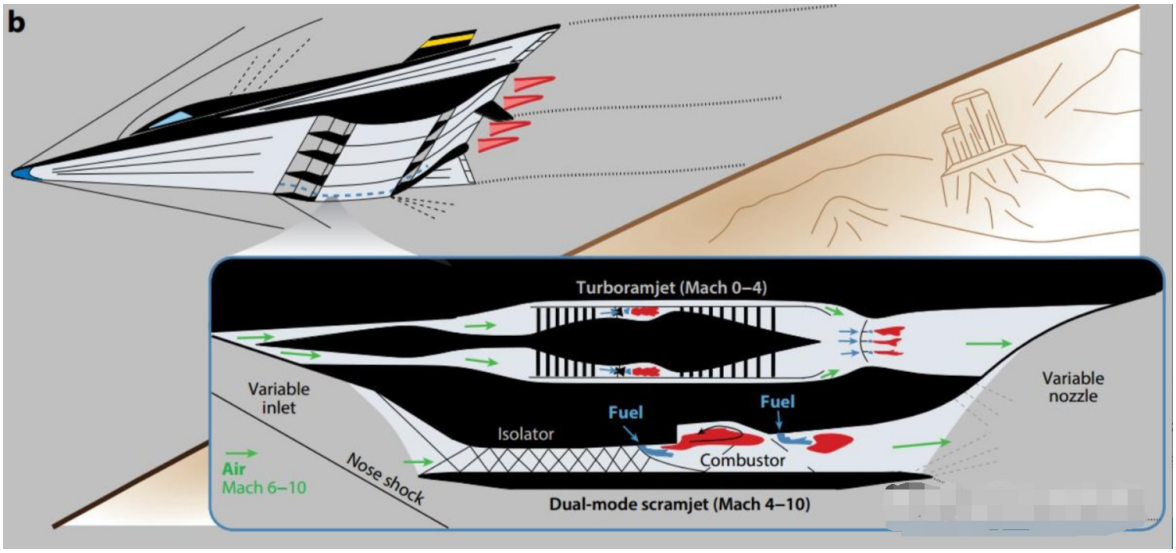

Figure 4.2 – A hybrid engine

4.3 Reach hypersonic speed

Future SSBJ are bound to fly even faster, to hypersonic speeds. Hypersonic aircraft (winged and wingless aircraft flying M number more than 5 times the speed of sound) is the strategic development direction of future military and civilian aircraft, known as the third revolution in aviation history after propeller and turbojet propulsion aircraft. With the further development of technology, the speed of SSBJ is bound to get faster and faster.[9][14]

Figure 4.3 – Hypersonic passenger aircraft concept

4.4 Aerodynamic arrangement of twin wings

In the 1930s, German scientist Adolf. Bazerman proposed the concept of Bazerman wing. He planned the traditional rhomboidal single wing from the string line to look like a flat triangle from the side, then reversed it and arranged the triangle's top Angle in symmetry to the top Angle to form a two-wing structure.

At present, the research of advanced scientists shows that under certain conditions, the aerodynamic arrangement of twin wings will make the air flow interfere with each other, so as to reduce the aerodynamic noise during supersonic cruise.

Bazerman’s biplane design not only promises to make supersonic travel a reality, but the biplane, which is cheaper, quieter and more energy efficient, is expected to become the mainstream solution for future supersonic aircraft.

Figure 4.4 – Biplane effect drawing

Reference

[1] Li Weiji.” General aircraft design.” Northwestern Polytechnical University Press, 2009.

[2] Jin Qi.” Supersonic business jet is not a dream.” Business jets and business flights, 2003,12, Vol. 34: 43-45.

[3] Paul Jackson.” Jean’s All the Worlds Aircraft.” ISBN-100710627920.

[4] John M. Swibart.” American aviation research and development goal - supersonic transport aircraft, bridge to the next century.” ISABE87-7087.

[5] Ang Haisong, Yu Xiongqing.” Advanced aircraft design technology.” National Defense Industry Press, 1983,06.

[6] Jia Yan.” Space civil aviation in the 21st century.” NEAT,1998.

[7] Dan dan.” Discussion on Sonic Boom calculation and Layout of supersonic business aircraft.” Aeronautical engineering progress, 2012.02.

[8] Tang wei.” Aerodynamic Design and Optimization for a wing-Body Vehicle, China Aerodynamic Research and Development Center, 2007.

[9] Shao Yuhong,” NASA's X-series hypersonic aircraft survey.” The 14th Research Institute of China Electronics Technology Group Corporation, 2010.

[10] A.K. Myalitsa, L.A. Malashenko, A.G. Grebenikov， E.T. Vasilevskiy, B.N. Klimenko, A.A. Serdyukov.” Development of a pilot project of an aircraft.” Kharkiv“KhAI”2011.

[11] Hu Tianyuan.” Research on Overall multidisciplinary Design Optimization of aircraft.” Nanjing University of Aeronautics and Astronautics, 2010.

[12] Zhang Yaozhong.” Aero pneumatic Manual.” National Defense Industry Press, 1983.06.

[13] Li Xulai.” New military transport aircraft for the 21st century.” Aircraft design references, 2002, Vol. 03.

[14] Li Wenliang.” The US Air Force's new generation supersonic cruise bomber.” Modern military. 2002.

[15] Ji Fengxian.” Study on aircraft wing profile Optimization Design.” Jiangxi Hongdu Group. 2000.

[16] Zhang Yanzhong.” Development of general aerodynamic technology for large aircraft.” Aviation Industry Corporation of China. 2008.

[17] Liebeck R H.” Design of the blended wing body subsonic transport. Journal of aircraft. 2004.

[18] Li Hua.” Aerodynamics Design of a wing-body Fusion Civil Transport Aircraft.” National University of Defense Technology, 2005.

[19] Zhu Ziqiang.” A new layout form of civil aircraft, wing-body fusion aircraft.” Beihang University, 2008.

[20] Zhao Qunli.” The development of military transport aircraft and its implications for us, 2002.

[21] Daniel P. Raymer.” Aircraft Design: A conceptual approach.” AIAA education series, American institute of Aeronautics and Astronautics, Inc. 1999.

[22] Hess, R.W.” Airframe cost estimating relationships.” R-3255-AF, Santa Monica, CA,1987.

[23] S Eyi, K.D. Lee.” Inverse Airfoil design using the Navier- Stokes equations, AIAA 1993-0972.

[24] S Wakayama.” Blended wing body Optimization of wing and wing body configurations using control theory, AIAA 1995-0123.

[25] Reuther J, Jameson A, Aerodynamic shape optimization of wing and wing body configurations using control theory, AIAA 1995-0132.

[26] J Blazek.” Computational fluid dynamics: Principles and applications.” Elsevier, 2001.

[27] B Mialon, T Fol, C Bonnaud.” Aerodynamic Optimization of Subsonic Flying Wing Configurations. AIAA: 2002-2931.

[28] Wilcox DC. Turbulence for Modeling for CFD. California DCW industries. Inc, 1993.

[29] Bald Win M.S.” Thin-layer Approximation and Algebraic Model for Separated Flows. AIAA,78-257, 1978.

[30] Andrea Aprovitola.” Stratospheric Ozone and Climate Forcing Sensitivity to Cruise Altitudes for Fleets of Potential Supersonic Transport Aircraft”. Journal of Geophysical Research: Atmospheres. 2021.

[31] R. Jones.” On the use of supersonic particle deposition to restore the structural integrity damaged aircraft structures Fatigue.” 2011

[32] F. Jivraj, R. Varvill.” The Scimitar Precooled Mach 5 Engine.” UK von Karman Institute for Fluid Dynamics, 2ND EUROPEAN CONFERENCE FOR AEROSPACE SCIENCES (EUCASS).